

A one-step spatial+ approach to mitigate spatial confounding in multivariate spatial areal models

Urdangarin, A.^{1,2}, Goicoa, T.^{1,2}, Kneib, T.³, Ugarte, M.D.^{1,2*}

¹ Department of Statistics, Computer Science, and Mathematics, Public University of Navarre, Spain.

² INAMAT², Public University of Navarre, Spain.

³ Georg-August-University of Göttingen, Chairs of Statistics and Econometrics, Germany

*Corresponding author: María Dolores Ugarte, Department of Statistics, Computer Science, and Mathematics, Public University of Navarre, Campus de Arrosadia, 31006 Pamplona, Spain.

E-mail: lola@unavarra.es

Abstract

Ecological spatial areal models encounter the well-known and challenging problem of spatial confounding. This issue makes it arduous to distinguish between the impacts of observed covariates and spatial random effects. Despite previous research and various proposed methods to tackle this problem, finding a definitive solution remains elusive. In this paper, we propose a one-step version of the spatial+ approach that involves dividing the covariate into two components. One component captures large-scale spatial dependence, while the other accounts for short-scale dependence. This approach eliminates the need to separately fit spatial models for the covariates. We apply this method to analyze two forms of crimes against women, namely rapes and dowry deaths, in Uttar Pradesh, India, exploring their relationship with socio-demographic covariates. To evaluate the performance of the new approach, we conduct extensive simulation studies under different spatial confounding scenarios. The results demonstrate that the proposed method provides reliable estimates of fixed effects and posterior correlations between different responses.

Keywords: Crimes against women; M-models; Spatial confounding; Spatial+.

1 Introduction

Univariate spatial models for areal count data have been a prevailing approach in smoothing standardized incidence or mortality ratios of chronic diseases. Though these techniques have been mainly applied to study incidence and mortality of different types of cancer, other applications exist. A very interesting one is the study of crimes against women in India (see Vicente et al., 2020a) where gender based violence is an issue. Univariate modelling is crucial for visualizing the spatial patterns of crimes against women. However, adopting a multivariate approach can enhance the accuracy of estimates and reveals latent correlations between the spatial patterns of crimes (Vicente et al., 2023b). This is essential for gaining a better understanding of this complex and multifaceted problem, and ultimately, for effective prevention.

Despite the substantial growth in research on multivariate spatial models for areal count data, their practical application is still limited due to the computational complexity involved in their implementation. While various approaches exist for constructing multivariate models for disease mapping (see for example MacNab, 2018), this study follows the corregionalization framework (Jin et al., 2007). In particular, the research by Martinez-Beneito (2013) presents a comprehensive

corregionalization approach that encompasses most of the multivariate methodologies suggested in the existing literature. However, this approach can be computationally prohibitive and an alternative reformulation known as M-models (Botella-Rocamora et al., 2015) is considered.

Incorporating potential risk factors (covariates) into a multivariate spatial model is important to evaluate the potential relationship between the covariates and the individual responses. This can contribute to gain knowledge about crimes against women, a multifaceted problem affected by social, religious, or economic characteristics with intricate interactions difficult to disentangle. However, when both, the covariate and spatial random effects enter in the model, an important challenge appears. Namely, how to separate the fixed effects from the spatial random effects. This is known as “spatial confounding”. When spatial random effects enter in the model, a change in the fixed effect estimates is observed compared to a simple linear or generalized linear model (GLM) that does not consider spatial correlation. Although spatial confounding has usually been considered as a collinearity problem between fixed effects and spatial random effects (see for instance Reich et al., 2006; Hodges & Reich, 2010; Hughes & Haran, 2013; Hanks et al., 2015; Page et al., 2017; Adin et al., 2023), there is not a unique general definition neither a unique solution. In fact, Gilbert et al. (2022) identify four different but related phenomena commonly referred as spatial confounding. In what follows, we consider that the effect of the unobserved covariates is approximated by spatial random effects in the model (Congdon, 2013; Marques et al., 2022), and we seek procedures that can simultaneously avoid bias in the estimates of the fixed effects, reduce their variance, and appropriately smooth the relative risks.

Various procedures have been proposed in the literature to address spatial confounding in the univariate framework, with restricted spatial regression (RSR) (Reich et al., 2006) being the most extended approach. RSR effectively deals with the collinearity between the covariate and spatial random effects by constraining the spatial random effects to lie in the orthogonal complement of the space spanned by the covariates. As a result, RSR provides fixed effects estimates that are equivalent to those obtained using a simple GLM. Additionally, the variance of the RSR fixed effects estimates falls somewhere between the variance obtained with the simple GLM and the variance obtained with the classical disease mapping spatial model (Reich et al., 2006; Hodges & Reich, 2010). Consequently, RSR might help prevent variance inflation of the fixed effects estimates, a concern that is widely recognized in spatial modelling. However, recent evidence contradicts some prior beliefs about RSR. Khan & Calder (2022) demonstrate that for normal responses, the variance of the fixed effects estimated with RSR is either equal to or lower than the variance obtained from the model without spatial random effects, leading to overly liberal inference. These authors also highlight potential issues of RSR for count data. Additionally, Gilbert et al. (2022) argue that RSR implicitly assumes the absence of unobserved covariates that overlap with the observed ones, as it forces the random effects to be orthogonal to the fixed effects. Furthermore, they support that the collinearity between the covariate and spatial random effects may not be a concern, but something expected if we assume the existence of unobserved covariates.

The spatial+ approach (Dupont et al., 2022) appears to be a promising method among the various alternatives for addressing spatial confounding. This is a two-step procedure that consists in removing spatial dependence from the covariate in a first step by fitting a spatial model to the covariate itself. Then, in the second step, a classical spatial regression model for the outcome is fitted replacing the covariate by the residuals obtained in the first step. In the univariate case, Urdangarin et al. (2023) conducted simulations to compare the fixed effects estimates of various approaches, including a simple GLM, the classical spatial model, the spatial+ approach, as well as other proposals such as RSR and transformed Gaussian Markov random fields (TGMRF) (Prates

et al., 2015). Overall, the spatial+ method demonstrated superior performance in terms of fixed effect estimates. Recent procedures to deal with spatial confounding include spectral methods (Guan et al., 2022), and a joint Gaussian Markov random field model for the covariate and the response (see Marques et al., 2022).

This work has two main objectives: firstly, we aim to propose a modified spatial+ approach to fit spatial models alleviating spatial confounding in a single step process. This approach eliminates the need to separately fit spatial models for the covariates. Secondly, we seek to estimate the latent correlations between several responses. To deal with these two goals we use M-models incorporating the modified spatial+ method that offer a tailored approach by accommodating the inclusion of distinct covariates for each individual response. Moreover, these models provide the necessary flexibility to effectively address spatial confounding for each response. To illustrate the procedure, we analyse crimes against women, rapes and dowry deaths, in the districts of Uttar Pradesh in 2011 and we assess their relationship with some sociodemographic covariates. To examine how well our proposal recovers the fixed effects and the correlations between crimes, we have simulated several scenarios under spatial confounding. The data generating model includes one observed covariate that has a distinct regression coefficient for each individual response and additional variability. Model fitting and inference is carried out from a full Bayes approach, using integrated nested Laplace approximations (Rue et al., 2009).

The rest of the article is organized as follows. In Section 2 we present the modified spatial+ to fit spatial models (univariate or multivariate) in a one-step procedure. Section 3 reviews the multivariate spatial models making emphasis on the M-models. Section 4 discusses some model implementation details and identifiability constraints. In Section 5 we use the procedures to analyse two crimes against women, rape and dowry death, in Uttar Pradesh, India, in the year 2011. Section 6 presents an exhaustive simulation study. Finally, the paper ends with a discussion.

2 One step spatial+ approach

The spatial+ method (Dupont et al., 2022) is a two step procedure designed to reduce bias in univariate spatial models by eliminating the spatial dependence of the covariates. The first step consists in fitting a spatial model to the covariate to remove the spatial dependence. Then, in the second step, the spatial model is fitted replacing the covariate by the residuals obtained in the first step. Here, we modify the spatial+ procedure to remove the spatial dependence of the covariate and fit the model in a one single step procedure. In fact, we will extend the spatial+ approach to the multivariate framework.

Let us consider the following univariate spatial disease mapping model where, conditional on the relative risk r_i , the number of counts in a given area $i = 1, \dots, n$, is assumed to follow a Poisson distribution

$$Y_i|r_i \sim \text{Poisson}(\mu_i = e_i r_i), \\ \log \mu_i = \log e_i + \log r_i,$$

where e_i are the number of expected counts. The log risk is modeled as

$$\log r_i = \alpha + \beta x_i + \theta_i,$$

where x_i is value of the covariate \mathbf{X} in the i -th area. In matrix form

$$\log \mathbf{r} = \mathbf{1}_n \alpha + \mathbf{X} \beta + \boldsymbol{\theta}, \quad (1)$$

where $\mathbf{r} = (r_1, \dots, r_n)'$, $\mathbf{1}_n$ is a column vector of ones of length n , $\mathbf{X} = (x_1, \dots, x_n)'$ and $\boldsymbol{\theta} = (\theta_1, \dots, \theta_n)'$ is the vector of spatial random effects with precision matrix $\boldsymbol{\Omega}$, which may be different depending on the spatial prior used for $\boldsymbol{\theta}$. In this paper we consider one of the following priors: intrinsic conditional autoregressive (ICAR) prior (Besag, 1974), proper conditional autorregressive (PCAR) prior (see for example Banerjee et al., 2015, chapter 4) or BYM2 prior (Riebler et al., 2016). In more detail, $\boldsymbol{\theta} \sim N(\mathbf{0}, \boldsymbol{\Omega})$, where the precision matrix $\boldsymbol{\Omega}$ depends on the spatial prior chosen:

- **ICAR:** $\boldsymbol{\Omega} = \tau(\mathbf{D} - \mathbf{W}) = \tau\mathbf{Q}$ where \mathbf{D} is a diagonal matrix with the number of neighbours of each area in the main diagonal and $\mathbf{W} = (w_{il})$ is a binary adjacency matrix where each entry w_{il} takes value 1 if areas i and l are neighbours and 0 otherwise. τ is the precision parameter. Note that \mathbf{Q} is the usual neighbourhood matrix where the i th diagonal element is equal to the number of neighbours of the area i , and the off diagonal elements $\mathbf{Q}_{il} = -1$ if the areas i and l share a common border and 0 otherwise.
- **PCAR:** $\boldsymbol{\Omega} = \tau(\mathbf{D} - \rho\mathbf{W})$, which provides a valid distribution if and only if $1/d_{min} < \rho < 1/d_{max}$ being d_{min} and d_{max} the minimum and maximum eigenvalues of $\mathbf{D}^{-1/2}\mathbf{W}\mathbf{D}^{-1/2}$ (Jin et al., 2007). When $\rho = 1$, the PCAR becomes the ICAR prior.
- **BYM2:** $\boldsymbol{\Omega} = \tau[(1 - \lambda)\mathbf{I}_n + \lambda\mathbf{Q}_*^-]^{-1}$ where \mathbf{I}_n is an $n \times n$ identity matrix and \mathbf{Q}_*^- is the Moore-Penrose generalized inverse of scaled precision matrix \mathbf{Q} (for more details see Riebler et al., 2016). In this prior, $0 \leq \lambda \leq 1$ represents the proportion of the marginal variance explained by the structured effect.

The spatial+ approach assumes that the covariate \mathbf{X} is modelled as

$$\mathbf{X} = \mathbf{f}(\mathbf{s}_1, \mathbf{s}_2) + \boldsymbol{\epsilon} \quad (2)$$

where $(\mathbf{s}_1, \mathbf{s}_2)$ are the coordinates (longitude and latitude) of the centroid of the small areas, $\mathbf{f}(\mathbf{s}_1, \mathbf{s}_2) = (f(s_{11}, s_{12}), f(s_{21}, s_{22}), \dots, f(s_{n1}, s_{n2}))'$ is a smooth function to be estimated using thin plate splines, and $\boldsymbol{\epsilon} \sim N(\mathbf{0}, \sigma_{\mathbf{X}}^2 \mathbf{I}_n)$, where $\sigma_{\mathbf{X}}$ is the standard deviation of the independent and identically distributed errors. The residuals of this model are defined as $\hat{\boldsymbol{\epsilon}} = \mathbf{X} - \hat{\mathbf{f}}(\mathbf{s}_1, \mathbf{s}_2)$ and the spatial model (1) is fitted replacing the covariate of interest \mathbf{X} by the residuals $\hat{\boldsymbol{\epsilon}}$.

Urdangarin et al. (2023) suggest an alternative to model (2) to remove the spatial dependence in the covariate. It consists in fitting a linear model where the response is now the covariate \mathbf{X} , and some of the eigenvectors of the spatial precision matrix \mathbf{Q} act as regressors. Each eigenvector captures spatial dependence at different scales, the eigenvectors corresponding to the lowest non-null eigenvalues being the smoothest ones. Thus, the number of eigenvectors included as covariates in the model defines the quantity of spatial dependence removed from \mathbf{X} . The simulation study performed by these authors indicates that with the new approach the fixed effects are recovered better than using thin plate splines. However this approach is also conducted in two steps.

In this paper, we introduce a one-step spatial+ approach without the need of fitting a spatial model to the covariate. The one-step spatial+ approach is a simpler and more straightforward procedure. Consider the spectral decomposition of the spatial precision matrix, $\mathbf{Q} = \mathbf{U}\Delta\mathbf{U}'$, where $\mathbf{U} = (\mathbf{U}_1, \dots, \mathbf{U}_n)$ is a orthogonal matrix whose columns are the eigenvectors of \mathbf{Q} and Δ is a $n \times n$ diagonal matrix with the eigenvalues of \mathbf{Q} in the main diagonal. Note that for connected graphs $\mathbf{U}_n = \mathbf{1}_n$ up to a normalizing constant and $\Delta_{nn} = 0$. Since the eigenvectors of \mathbf{Q} form a basis of \mathbb{R}^n and contain spatial information at different scales, we now express the covariate \mathbf{X} as a linear combination of the eigenvectors \mathbf{U}_i , $i = 1, \dots, n$, that is,

$$\mathbf{X} = a_1\mathbf{U}_1 + \dots + a_n\mathbf{U}_n.$$

Given that the eigenvectors corresponding to the lowest non-null eigenvalues are responsible for the collinearity between the fixed and random effects, we split the covariate into two parts

$$\mathbf{X} = \mathbf{Z} + \mathbf{Z}^*, \quad (3)$$

where $\mathbf{Z}^* = a_{n-k}\mathbf{U}_{n-k} + \dots + a_n\mathbf{U}_n$ comprises large-scale eigenvectors associated with the lowest eigenvalues, $\mathbf{Z} = a_1\mathbf{U}_1 + \dots + a_{n-(k+1)}\mathbf{U}_{n-(k+1)}$ contains the rest of eigenvectors, and k is the number of large-scale eigenvectors assigned to \mathbf{Z}^* . Finally, the spatial model (1) is fitted replacing the covariate \mathbf{X} by its spatially decorrelated part \mathbf{Z} as

$$\log \mathbf{r} = \mathbf{1}_n \alpha + \mathbf{Z} \beta + \boldsymbol{\theta}. \quad (4)$$

We have verified that the spatial+ proposed in Urdangarin et al. (2023) and the one-step spatial+ proposed here yield to almost identical results in univariate models.

In the next section, we introduce multivariate disease mapping models and extend the modified spatial+ approach to this framework.

3 Multivariate ecological spatial areal models

Multivariate spatial areal models handle two types of dependencies: within-response dependence, often characterized by spatial dependence, and between-response correlations, which typically lack of a specific structure and pose a challenge. Multivariate models, in general, have the potential to provide more reliable risk estimates compared to traditional univariate models. In this paper, we employ multivariate ecological regression models to examine potential linear associations between the responses and a covariate of interest.

Let now Y_{ij} and e_{ij} denote, respectively, the number of observed and expected cases in the i th small area ($i = 1, \dots, n$) and j th crime ($j = 1, \dots, J$), and assume that Y_{ij} follows a Poisson distribution conditioned on the relative risk r_{ij} , that is

$$Y_{ij}|r_{ij} \sim \text{Poisson}(\mu_{ij} = e_{ij}r_{ij}), \\ \log \mu_{ij} = \log e_{ij} + \log r_{ij}.$$

The log-risk is modeled as

$$\log r_{ij} = \alpha_j + \beta_j x_i + \theta_{ij} \quad (5)$$

where α_j is the intercept of j th crime, β_j is a crime-specific regression coefficient related to the covariate $\mathbf{X} = (x_1, \dots, x_n)'$ and θ_{ij} is the spatial effect of area i and crime j . Model (5) can be expressed in matrix form as

$$\log \mathbf{r} = (\mathbf{I}_J \otimes \mathbf{1}_n)\boldsymbol{\alpha} + (\mathbf{I}_J \otimes \mathbf{X})\boldsymbol{\beta} + \boldsymbol{\theta} \quad (6)$$

where $\mathbf{r} = (r'_1, \dots, r'_J)'$ is the vector of relative risks with $\mathbf{r}_j = (r_{1j}, \dots, r_{nj})'$ for $j = 1, \dots, J$, \mathbf{I}_J is a $J \times J$ identity matrix and $\mathbf{1}_n$ is a vector of ones of length n . The vectors of crime-specific intercepts and regression coefficients are denoted by $\boldsymbol{\alpha} = (\alpha_1, \dots, \alpha_J)'$ and $\boldsymbol{\beta} = (\beta_1, \dots, \beta_J)'$ respectively. Finally, $\boldsymbol{\theta} = (\theta'_1, \dots, \theta'_J)'$ where $\boldsymbol{\theta}_j = (\theta_{1j}, \dots, \theta_{nj})'$ is the vector of spatial random effects of the j th crime. The within and between-crimes dependence is introduced through the precision/covariance

matrix of the spatial random effect. In particular the following prior distribution with Gaussian kernel $p(\boldsymbol{\theta}) \propto \exp\left(-\frac{1}{2}\boldsymbol{\theta}'\boldsymbol{\Omega}_{\boldsymbol{\theta}}\boldsymbol{\theta}\right)$ is considered for $\boldsymbol{\theta}$, where

$$\boldsymbol{\Omega}_{\boldsymbol{\theta}} = (\mathbf{M}^{-1} \otimes \mathbf{I}_n) \text{Blockdiag}(\boldsymbol{\Omega}_1, \dots, \boldsymbol{\Omega}_J) (\mathbf{M}^{-1} \otimes \mathbf{I}_n)' . \quad (7)$$

Note that \mathbf{M} is any square root of the between-crime covariance matrix $\boldsymbol{\Sigma}_b$, and $\boldsymbol{\Omega}_j$ are the spatial precision matrix for the j crime. Here $\boldsymbol{\Omega}_j$ can be the precision matrix of the ICAR, PCAR or BYM2 priors. For the ICAR prior, the precision matrix is the same for all crimes and $\boldsymbol{\Omega}_{\boldsymbol{\theta}}$ has a separable structure, $\boldsymbol{\Omega}_{\boldsymbol{\theta}} = \boldsymbol{\Sigma}_b^{-1} \otimes (\mathbf{D} - \mathbf{W})$. Likewise, for the PCAR and BYM2 priors, if $\rho_j = \rho$ and $\lambda_j = \lambda$ for $j = 1, \dots, J$, we have the separable precision matrices $\boldsymbol{\Omega}_{\boldsymbol{\theta}} = \boldsymbol{\Sigma}_b^{-1} \otimes (\mathbf{D} - \rho \mathbf{W})$ and $\boldsymbol{\Omega}_{\boldsymbol{\theta}} = \boldsymbol{\Sigma}_b^{-1} \otimes [(1 - \lambda)\mathbf{I}_n + \lambda \mathbf{Q}_*]^{-1}$, respectively.

In the following, we review how to introduce spatial dependencies within crimes as well as the correlation between spatial patterns of different crimes through the M-models (Botella-Rocamora et al., 2015). In this paper, the multivariate models include a single covariate, but the proposed methodology can be extended to the case of multiple covariates.

To better understand how the M-models deal with the within and between-crime dependence, we rearrange the spatial effects into the matrix $\boldsymbol{\Theta} = (\boldsymbol{\theta}_1, \dots, \boldsymbol{\theta}_J) = \{\theta_{ij} : i = 1, \dots, n; j = 1, \dots, J\}$. Following Botella-Rocamora et al. (2015), $\boldsymbol{\Theta}$ can be expressed as

$$\boldsymbol{\Theta} = \boldsymbol{\Phi} \mathbf{M} \quad (8)$$

where the columns of the matrix $\boldsymbol{\Phi} = (\boldsymbol{\Phi}_1, \dots, \boldsymbol{\Phi}_J)$ are independent and follow a spatially correlated distribution to deal with spatial dependence within crimes. The $J \times J$ matrix \mathbf{M} induces dependence between the columns of $\boldsymbol{\Phi}$, that is, it induces correlation between the spatial patterns of different crimes. A typical election for \mathbf{M} is to consider the lower triangular matrix of the Cholesky decomposition of the between-crime covariance matrix $\boldsymbol{\Sigma}_b$, however it can induce dependence on the order of the crimes (Martinez-Beneito, 2013). To avoid this undesired situation, \mathbf{M} is any nonsingular but arbitrary matrix. Using that

$$\text{vec}(\mathbf{ABC}) = (\mathbf{C}' \otimes \mathbf{A})\text{vec}(\mathbf{B}),$$

(see for example Harville, 2008, p. 345) where the vec operator stacks the columns of a matrix one under the other and \mathbf{A} , \mathbf{B} , and \mathbf{C} are conformable matrices for multiplication, it is obtained that

$$\text{vec}(\boldsymbol{\Theta}) = \boldsymbol{\theta} = (\mathbf{M}' \otimes \mathbf{I}_n)\text{vec}(\boldsymbol{\Phi}).$$

Then, the covariance matrix of $\boldsymbol{\theta}$ is

$$\begin{aligned} \text{cov}(\boldsymbol{\theta}) &= (\mathbf{M} \otimes \mathbf{I}_n)' \text{cov}(\text{vec}(\boldsymbol{\Phi})) (\mathbf{M} \otimes \mathbf{I}_n) = \\ &= (\mathbf{M} \otimes \mathbf{I}_n)' \text{Blockdiag}(\boldsymbol{\Sigma}_1, \dots, \boldsymbol{\Sigma}_J) (\mathbf{M} \otimes \mathbf{I}_n), \end{aligned}$$

where $\boldsymbol{\Sigma}_j$ is the spatial covariance matrix or each of the columns of $\boldsymbol{\Phi}$. Clearly, the inverse of this matrix is the precision matrix $\boldsymbol{\Omega}_{\boldsymbol{\theta}}$ in equation (7).

To make the spatial random effects identifiable, appropriate sum-to-zero constraints must be contemplated. Here, we will consider the constraints proposed by Goicoa et al. (2018) for each crime. In addition, we fix the precision parameters of the spatial precision matrices equal 1 to make the entries of the \mathbf{M} matrix identifiable (Martinez-Beneito, 2013).

The covariance structure between the spatial patterns of different crimes can be estimated as $\Sigma_b = \mathbf{M}'\mathbf{M}$, and the entries of \mathbf{M} can be interpreted as coefficients in the regression of log-relative risks on the columns of Φ . Hence, they can be treated as fixed effects and assigning a zero-centered normal prior with large fixed variance is a reasonable choice. This is equivalent to assume a Wishart prior to Σ_b , i.e. $\Sigma_b = \mathbf{M}'\mathbf{M} \sim \text{Wishart}(J, \sigma^2 \mathbf{I}_J)$ (for more details see Botella-Rocamora et al., 2015).

Finally, to deal with spatial confounding, the multivariate M-model (6) is fitted replacing the covariate \mathbf{X} by its spatially decorrelated part \mathbf{Z} as

$$\log \mathbf{r} = (\mathbf{I}_J \otimes \mathbf{1}_n)\boldsymbol{\alpha} + (\mathbf{I}_J \otimes \mathbf{Z})\boldsymbol{\beta} + \boldsymbol{\theta}. \quad (9)$$

Note that Model (9) allows removing a different number of eigenvectors for each crime. That is

$$\log \mathbf{r} = (\mathbf{I}_J \otimes \mathbf{1}_n)\boldsymbol{\alpha} + \begin{pmatrix} \mathbf{Z}_1 & \cdots & \mathbf{0} \\ \vdots & \ddots & \vdots \\ \mathbf{0} & \cdots & \mathbf{Z}_J \end{pmatrix} \boldsymbol{\beta} + \boldsymbol{\theta},$$

where \mathbf{Z}_j is the part of the covariate that we retain for crime $j = 1, \dots, J$.

4 Model implementation

In this paper, models are fitted using the Integrated nested Laplace approximation (INLA) approach (Rue et al., 2009). INLA is designed for approximate Bayesian inference avoiding the convergence issues of MCMC techniques and saving computing time. Hence it has become very popular for performing Bayesian inference with a wide range of hierarchical models. The R package **R-INLA** (Lindgren & Rue, 2015) has many models directly available and allows to implement other models using **rgeneric** or **cgeneric** constructions. The M-models are not directly available in **R-INLA**, so here we will use the **rgeneric** construction as in Vicente et al. (2020b).

The matrix \mathbf{M} involves $J \times J$ parameters when only $J \times (J + 1)/2$ parameters are needed to determine the covariance matrix $\Sigma_b = \mathbf{M}'\mathbf{M}$. Thus, to avoid overparameterization, when we consider the Wishart prior on the covariance matrix, $\Sigma_b = \mathbf{M}'\mathbf{M} \sim \text{Wishart}(J, \sigma^2 \mathbf{I}_J)$, we use the Bartlett decomposition of Wishart distributed matrices (see for example Peña & Irie, 2022). More precisely, if $\Sigma_b \sim \text{Wishart}(\nu, \mathbf{V})$, the Bartlett decomposition of Σ_b is $\Sigma_b = \mathbf{L}\mathbf{A}\mathbf{A}'\mathbf{L}'$. Here \mathbf{L} is the Cholesky factor of \mathbf{V} and

$$\mathbf{A} = \begin{bmatrix} c_1 & 0 & 0 & \cdots & 0 \\ n_{21} & c_2 & 0 & \cdots & 0 \\ n_{31} & n_{32} & c_3 & \cdots & 0 \\ \vdots & \vdots & \vdots & \ddots & \vdots \\ n_{J1} & n_{J2} & n_{J3} & \cdots & c_J \end{bmatrix}, \quad (10)$$

where the diagonal and non-diagonal elements are independently distributed as $c_j \sim \chi_{\nu-j+1}$ and $n_{jl} \sim N(0, 1)$ for $j, l = 1, \dots, J$ with $j > l$. Using the Bartlett decomposition we only use $J \times (J + 1)/2$ parameters instead of $J \times J$ parameters. In our case, $\mathbf{V} = \mathbf{I}_J$ and then $\mathbf{L} = \mathbf{I}_J$. Finally, to avoid dependence with the order of the crimes, we consider \mathbf{M} in Equation (7) as the eigen-decomposition of Σ_b . Details about the implementation of the Bartlett decomposition can be found in Vicente et al. (2023a).

Finally, we have considered a uniform distribution $\text{Unif}(0,1)$ for the hyperparameters ρ_j and λ_j of the PCAR and BYM2 spatial priors. Note that the $\text{Unif}(0,1)$ prior on the parameters ρ_j is used to consider only positive spatial correlations (see for example Martínez-Beneito & Botella-Rocamora, 2019, Chap. 4, p.147). A normal distribution with mean 0 and precision 0.001 are given to crime-specific intercepts α_j and regression coefficients β_j . All the models are fitted using R-INLA package version 22.12.16 (dated 2022-12-23) with the simplified laplace strategy. The full code and data to reproduce results will be available at https://github.com/spatialstatisticupna/Multivariate_confounding.

5 Illustration: joint analysis of rapes and dowry deaths in Uttar Pradesh in 2011

In this section we analyse jointly rapes and dowry deaths, two forms of crimes against women in the 70 districts of Uttar Pradesh in 2011. The main objective is to assess whether there is linear association between a covariate of interest and the relative risks of each crime using the multivariate models with the spatial+ approach defined in the previous sections.

Uttar Pradesh is the most populated state of India and it is located in the north of the country. Despite underreporting, the elevated number of rapes in India is a matter of concern (see Vicente et al., 2018, for the temporal evolution of rapes in Uttar Pradesh). Dowry death is deeply-rooted to the marriage system in India and it is related to the dowry. The dowry represents the goods that the bride's family offers to the groom's family before the marriage. Disputes related to the dowry are common and the use of violence against the bride in order to obtain a higher dowry is extended. Unfortunaly, this violence often ends in the dead of the woman. This is known as dowry death. Any death related to dowry, such as, murder or suicide of the woman within the first seven years of marriage is considered a dowry death (Vicente et al., 2020a). Although in 1961 the Dowry Prohibition Act was approved, the tradition of dowry is still widespread.

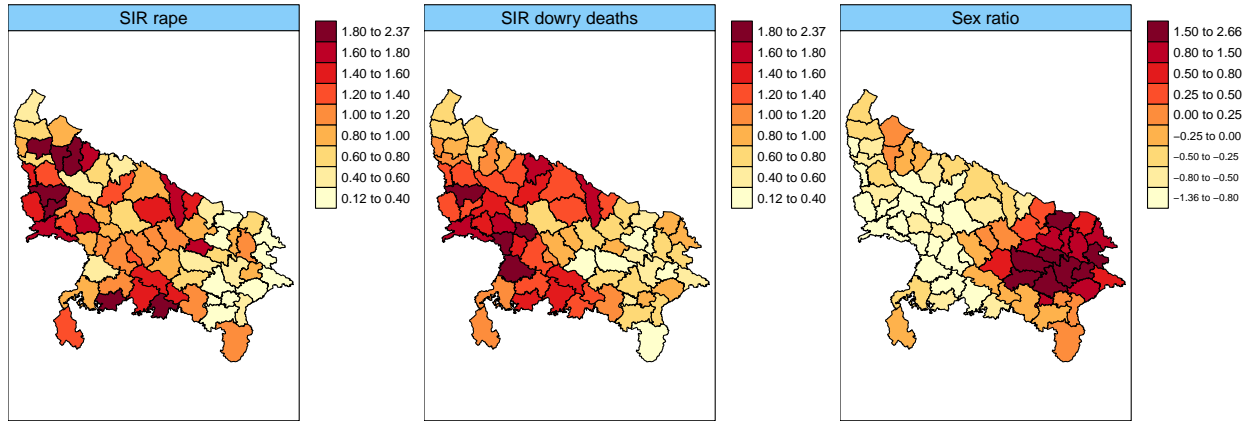


Figure 1: Standardized incidence ratio for rapes (left), dowry deaths (center), and the spatial pattern of sex ratio (right) in Uttar Pradesh in 2011.

The minimum values for rapes and dowry deaths in 2011 are 2 and 6 respectively, whereas the maximum values are 89 and 95. So, the number of rapes and dowry deaths per district in 2011 is highly variable. Figure 1 displays the standardized incidence ratio (SIR) of rapes and dowry deaths in 2011. Some similarities between both spatial patterns can be observed with a Pearson correlation coefficient of 0.4471. Thus, it is sensible to analyse both crimes jointly. Figure 1 also shows the spatial pattern of the (standardized) covariate sex ratio (X_1) defined as the number of females per

1000 males. Here, the goal is to assess the potential linear association between the sex ratio and the relative risks of rapes and dowry deaths. However, this task may not be straightforward due to the evident spatial pattern of the covariate sex ratio, and the addition of spatial random effects as a proxy of unobserved covariates can induce bias in the fixed effects estimates (spatial confounding).

Here we fit the M-models (6) and (9) introduced in Section 2. First, the covariate sex ratio is expressed as a linear combination of the eigenvectors of the precision matrix \mathbf{Q} (see Equation (3)). Then we remove \mathbf{Z}^* , the part of the linear combination containing the large scale eigenvectors associated with the k lowest eigenvalues. The number of large-scale eigenvectors chosen depends on the dimensions of \mathbf{Q} . Here, k is between 5 and 20, which represent 7% and 29% of all eigenvectors. Table 1 presents the notation of the M-models used. All the M-models are fitted considering ICAR, PCAR and BYM2 priors for the spatial random effects.

Table 1: Different proposals for the multivariate M-models fitted to the data. The column Covariate refers to the covariate included in the M-model, k indicates the number of large-scale eigenvectors of \mathbf{Q} that comprises \mathbf{Z}^* and $n - (k + 1)$ is the number of the rest of eigenvectors comprised in \mathbf{Z} .

Name	M-model	Covariate	k	$n - (k + 1)$
M-Spatial	(6)	\mathbf{X}_1	—	—
M-SpatPlus64	(9)	\mathbf{Z}	5	64
M-SpatPlus59	(9)	\mathbf{Z}	10	59
M-SpatPlus54	(9)	\mathbf{Z}	15	54
M-SpatPlus49	(9)	\mathbf{Z}	20	49

Table 2 provides posterior means, posterior standard errors and 95% credible intervals of sex ratio for rapes (β_1) and dowry deaths (β_2) with different M-models. A negative linear association is observed between sex ratio and both crimes. For rapes, the 95% credible intervals always contain 0 irrespective of the models and the spatial prior, indicating a non-significant relationship between rapes and sex ratio. For dowry deaths, we observed a reduction of the posterior mean in the spatial+ models with respect the spatial model. However, 95% credible intervals exclude 0 with the M-Spatial, the M-SpatPlus64 and the M-SpatPlus59 models. In general, multivariate models with the spatial+ approach reduce the posterior standard deviations in comparison to the usual multivariate spatial model. Overall, the three spatial priors lead to similar fixed effects estimates, though some differences appears in the multivariate spatial models without the spatial+. The results are in line with previous literature as dowry death is the only crime against women that seems to be associated with sex ratio (see for example Mukherjee et al., 2001).

Table 3 presents the posterior median of the correlation between rapes and dowry deaths with their 95% credible intervals. The estimated correlations are about 0.3 but slight discrepancies are noted in the estimates depending on the model and the spatial prior. Multivariate spatial+ models with PCAR prior points towards a significant correlation. However, the rest of models indicate that the correlation is not significant. Given that the lower bounds of the credible intervals are very close to zero, we might conclude that the correlation is on the verge of significance. Finally, to compare the models in terms of goodness of fit and complexity, we have computed the Deviance Information Criteria (DIC) and the Watanabe-Akaike Information Criterion (WAIC) (see Table 4). M-models with spatial+ improve slightly the fit compared to the M-Spatial model, but differences are negligible. This is expected as the spatial+ approach can be seen as a kind of reparameterization of the spatial model.

To summarize, different fixed effects are estimated for both crimes depending on the model fitted

Table 2: Posterior means, standard errors and 95% credible intervals of β_1 (rapes) and β_2 (dowry deaths) for Uttar Pradesh data in 2011.

		β_1				β_2			
		Model	Mean	SD	95% CI	Mean	SD	95% CI	
ICAR	M-Spatial	-0.1560	0.1050	-0.3630	0.0500	-0.1920	0.0600	-0.3080	-0.0720
	M-SpatPlus64	-0.0750	0.0680	-0.2090	0.0590	-0.0940	0.0410	-0.1730	-0.0130
	M-SpatPlus59	-0.0750	0.0640	-0.2010	0.0500	-0.0810	0.0390	-0.1580	-0.0040
	M-SpatPlus54	-0.0720	0.0580	-0.1860	0.0420	-0.0430	0.0370	-0.1150	0.0290
	M-SpatPlus49	-0.0870	0.0550	-0.1960	0.0210	-0.0460	0.0350	-0.1150	0.0230
PCAR	M-Spatial	-0.2270	0.0950	-0.4070	-0.0330	-0.2520	0.0570	-0.3600	-0.1350
	M-SpatPlus64	-0.0750	0.0690	-0.2100	0.0600	-0.0970	0.0430	-0.1830	-0.0130
	M-SpatPlus59	-0.0770	0.0650	-0.2060	0.0520	-0.0840	0.0410	-0.1640	-0.0030
	M-SpatPlus54	-0.0720	0.0590	-0.1890	0.0450	-0.0440	0.0390	-0.1200	0.0320
	M-SpatPlus49	-0.0870	0.0570	-0.1990	0.0240	-0.0460	0.0380	-0.1200	0.0270
BYM2	M-Spatial	-0.1800	0.0990	-0.3720	0.0150	-0.2500	0.0590	-0.3620	-0.1310
	M-SpatPlus64	-0.0680	0.0670	-0.2000	0.0650	-0.1100	0.0430	-0.1940	-0.0260
	M-SpatPlus59	-0.0720	0.0640	-0.1990	0.0550	-0.0960	0.0410	-0.1780	-0.0150
	M-SpatPlus54	-0.0710	0.0610	-0.1900	0.0480	-0.0490	0.0390	-0.1250	0.0270
	M-SpatPlus49	-0.0930	0.0590	-0.2080	0.0220	-0.0540	0.0380	-0.1280	0.0200

Table 3: Posterior medians and 95% credible intervals of estimated correlations between rapes and dowry deaths for Uttar Pradesh data in 2011.

		ICAR			PCAR			BYM2		
Model	Median	95% CI	Median	95% CI	Median	95% CI	Median	95% CI		
M-Spatial	0.3066	-0.0677	0.6087	0.3127	-0.0508	0.6177	0.2502	-0.1483	0.5703	
M-SpatPlus64	0.3376	-0.0090	0.6275	0.3698	0.0302	0.6503	0.3096	-0.0722	0.6499	
M-SpatPlus59	0.3320	-0.0151	0.6313	0.3601	0.0245	0.6361	0.3086	-0.0021	0.6079	
M-SpatPlus54	0.3347	-0.0056	0.6097	0.3713	0.0448	0.6304	0.2622	-0.0688	0.5869	
M-SpatPlus49	0.3222	-0.0185	0.6229	0.3657	0.0405	0.6245	0.2581	-0.0368	0.5464	

to the data. For rapes, the posterior mean of sex ratio coefficient β_1 is negative but the 95% credible intervals does not point toward a significant negative association. For dowry deaths, the conclusions depends on the number of large-scale eigenvectors excluded in M-models with spatial+. According to Urdangarin et al. (2023), in univariate spatial+ spatial models, removing 14% to 21% of eigenvectors could lead to unbiased fixed effect estimates. Here, M-SpatPlus59 and M-SpatPlus54 are the equivalent models to removing 14% and 21% of eigenvectors. The 95% credible interval of M-SpatPlus59 point toward a significant negative association between sex ratio and dowry deaths. Nevertheless, caution is recommended when reaching conclusions.

We have also run the models including other socioeconomic covariates. The results are omitted to save space. Among all the covariates analysed, only the covariate “number of burglaries” shows a significant positive linear association with rapes, but it does not show a significant association with dowry deaths. We have fitted all the previous M-models including both, sex ratio and burglaries as covariates but overall, the fixed effect estimates for each response do not change. The M-models proposed here allow removing different quantity of spatial dependence from each covariate, as well as the inclusion of specific covariates for a particular response. For example, the covariate burglary might be considered only for the analysis of rapes, while the sex ratio might be included only for

dowry deaths.

Table 4: DIC and WAIC for Uttar Pradesh data in 2011.

Model	ICAR		PCAR		BYM2	
	DIC	WAIC	DIC	WAIC	DIC	WAIC
M-Spatial	959.1602	949.0371	961.2425	948.8055	959.7526	946.1454
M-SpatPlus64	958.7318	945.9487	960.0558	944.6206	960.2536	943.0920
M-SpatPlus59	958.8249	945.6563	960.0255	944.4730	960.3539	942.8094
M-SpatPlus54	959.3916	945.3981	960.7766	944.4437	960.7177	943.4793
M-SpatPlus49	959.3160	945.5091	960.9914	944.7533	960.3658	943.0917

6 Simulation study

In this section, we conduct two simulation studies, named Simulation study 1 and Simulation study 2, to evaluate the performance of the spatial+ method in multivariate models in presence of spatial confounding. For both simulation studies, we have employed the geographical configuration of Uttar Pradesh consisting of 70 connected districts. Two related responses, denoted as crime 1 and crime 2 from now on, are generated. In Simulation study 1 we examine if the spatial+ method recovers the true fixed effects for each of the crimes when there is spatial confounding. Simulation Study 2 focuses on evaluating how well the multivariate models with spatial+ technique simultaneously estimate the correlation between crimes and the fixed effects.

Simulation study 1: the data generating model includes the standardized covariate sex ratio of the real data analysis, denoted as \mathbf{X}_1 , and two additional covariates, \mathbf{X}_2 and \mathbf{X}_3 . Both \mathbf{X}_2 and \mathbf{X}_3 play the role of unobserved covariates in the fitted model for crimes 1 and 2 respectively, and hence they can induce spatial confounding. The correlation between \mathbf{X}_2 and \mathbf{X}_3 , as well as the correlations between \mathbf{X}_1 and \mathbf{X}_2 and \mathbf{X}_1 and \mathbf{X}_3 are fixed. The fitted models do not include \mathbf{X}_2 and \mathbf{X}_3 . In more detail, the counts for crime 1 and crime 2 are simulated as follows,

$$\log \mathbf{r} = (\mathbf{I}_J \otimes \mathbf{1}_n) \boldsymbol{\alpha} + (\mathbf{I}_J \otimes \mathbf{X}_1) \boldsymbol{\beta} + \begin{pmatrix} \mathbf{X}_2 & \mathbf{0} \\ \mathbf{0} & \mathbf{X}_3 \end{pmatrix} \boldsymbol{\beta}^* \quad (11)$$

$$\mathbf{Y}^l | \mathbf{r} \sim Poisson(\boldsymbol{\mu} = \mathbf{e}\mathbf{r}) \quad (12)$$

where $\boldsymbol{\alpha} = (\alpha_1, \alpha_2)' = (-0.12, -0.03)', \boldsymbol{\beta} = (\beta_1, \beta_2)' = (-0.15, -0.20)', \boldsymbol{\beta}^* = (\beta_1^*, \beta_2^*)' = (-0.30, -0.30)', l = 1, \dots, L$, and \mathbf{e} is the vector of expected cases of the real case study. Two scenarios are simulated depending on the correlations between \mathbf{X}_1 , \mathbf{X}_2 and \mathbf{X}_3 . Scenario 1 addresses moderate-high correlations between the covariates and Scenario 2 moderate-low correlations.

- **Scenario 1:** the correlations are $cor(\mathbf{X}_1, \mathbf{X}_2) = 0.5$, $cor(\mathbf{X}_1, \mathbf{X}_3) = 0.7$ and $cor(\mathbf{X}_2, \mathbf{X}_3) = 0.7$. Here spatial confounding might be a major concern.
- **Scenario 2:** the correlations are $cor(\mathbf{X}_1, \mathbf{X}_2) = 0.3$, $cor(\mathbf{X}_1, \mathbf{X}_3) = 0.5$ and $cor(\mathbf{X}_2, \mathbf{X}_3) = 0.3$. In this case, spatial confounding might not be so severe.

Figure B.4 shows the standardized sex ratio covariate and simulated \mathbf{X}_2 and \mathbf{X}_3 covariates. The first row shows the spatial patterns of the covariates for Scenario 1 and the second row for Scenario 2. For each of the scenarios a total of $L = 300$ counts data sets are generated. To complete the

simulation study, Supplementary material A presents the details about the data generating process of some additional scenarios, Scenarios 3, 4, 5 and 6, and their results. (Note that in Scenarios 5 and 6, $\text{cor}(\mathbf{X}_1, \mathbf{X}_2) = 0$ and hence, confounding should not be an issue for crime 1.)

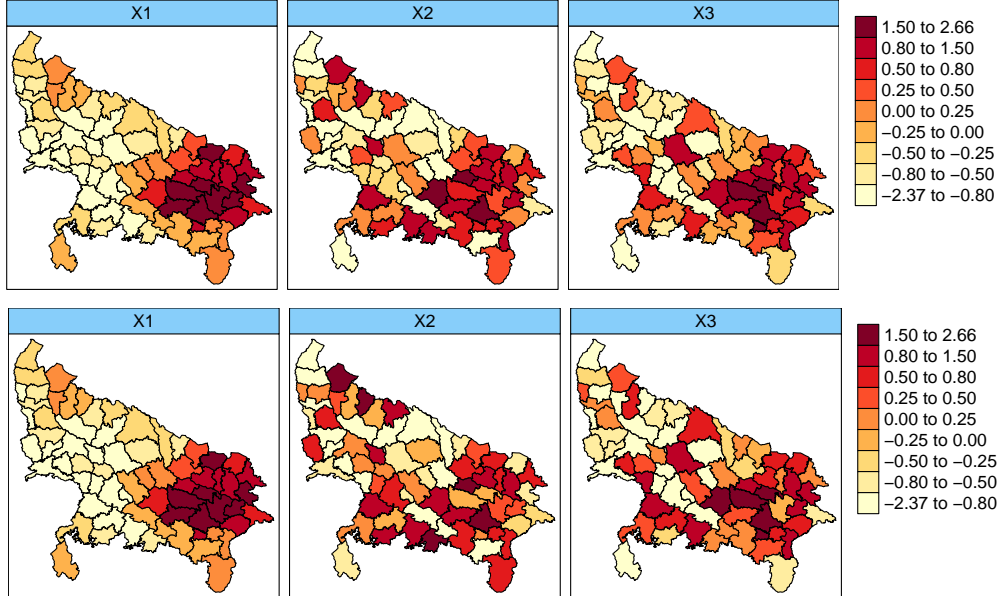


Figure 2: From left to right, standardized sex ratio covariate in 2011, standardized simulated covariate \mathbf{X}_2 and standardized simulated covariate \mathbf{X}_3 in Simulation Study 1. The top row corresponds to Scenario 1 and the bottom row to Scenario 2.

Simulation study 2: the aim of this simulation study is to see how well multivariate models with the spatial+ method estimate the fixed effects but also the correlation between crimes. The objective is to see whether the modified spatial+ method introduces some bias in the estimation of the between-crime correlations. Here, the data generating process is quite different to Simulation study 1. First, a vector of spatial effects, $\boldsymbol{\theta} = (\boldsymbol{\theta}'_1, \boldsymbol{\theta}'_2)'$ is generated as $\boldsymbol{\theta} \sim N(\mathbf{0}, \boldsymbol{\Omega}_{\boldsymbol{\theta}})$ where the precision matrix $\boldsymbol{\Omega}_{\boldsymbol{\theta}}$ follows the separable structure $\boldsymbol{\Omega}_{\boldsymbol{\theta}} = \boldsymbol{\Sigma}_b^{-1} \otimes (\mathbf{D} - \mathbf{W})$. The 2×2 covariance matrix between crimes, $\boldsymbol{\Sigma}_b$, is conveniently expressed as

$$\boldsymbol{\Sigma}_b = \begin{pmatrix} \sigma_1 & 0 \\ 0 & \sigma_2 \end{pmatrix} \begin{pmatrix} 1 & \rho \\ \rho & 1 \end{pmatrix} \begin{pmatrix} \sigma_1 & 0 \\ 0 & \sigma_2 \end{pmatrix}$$

where $\sigma_1^2 = 0.9$, $\sigma_2^2 = 0.2$ are the variances obtained with M-Spatial model in the real data analysis and ρ is the pre-defined linear correlation between crime 1 and crime 2. In a second step, a covariate \mathbf{X}_1^* is simulated such that its linear correlation with the spatial effects of crime 1, $\boldsymbol{\theta}_1$, and the spatial effects of crime 2, $\boldsymbol{\theta}_2$, is fixed. In more detail, data are generated as,

$$\log \mathbf{r} = (\mathbf{I}_J \otimes \mathbf{1}_n) \boldsymbol{\alpha} + (\mathbf{I}_J \otimes \mathbf{X}_1^*) \boldsymbol{\beta} + \boldsymbol{\theta} \quad (13)$$

$$\mathbf{Y}^l | \mathbf{r} \sim \text{Poisson}(\boldsymbol{\mu} = \mathbf{e}\mathbf{r}) \quad (14)$$

where $\boldsymbol{\theta} = (\boldsymbol{\theta}'_1, \boldsymbol{\theta}'_2)', l = 1, \dots, L$ and \mathbf{e} is the vector of expected cases of the real case study. In this case, $\boldsymbol{\alpha} = (\alpha_1, \alpha_2)' = (0.12, 0.03)'$ and $\boldsymbol{\beta} = (\beta_1, \beta_2)' = (0.15, 0.20)'$ are considered. Two scenarios are simulated depending on the correlation between crimes, ρ , and the correlations between the simulated \mathbf{X}_1^* and the spatial effects $\boldsymbol{\theta}_1$ and $\boldsymbol{\theta}_2$. Scenario 1 addresses moderate-high correlations and Scenario 2 deals with low-moderate correlations.

- **Scenario 1:** the correlations are $\rho = 0.7$, $\text{cor}(\mathbf{X}_1^*, \boldsymbol{\theta}_1) = 0.5$ and $\text{cor}(\mathbf{X}_1^*, \boldsymbol{\theta}_2) = 0.7$. Here spatial confounding might be a major concern and the crimes are highly correlated.
- **Scenario 2:** the correlations are $\rho = 0.3$, $\text{cor}(\mathbf{X}_1^*, \boldsymbol{\theta}_1) = 0.3$ and $\text{cor}(\mathbf{X}_1^*, \boldsymbol{\theta}_2) = 0.5$. In this case, spatial confounding might not be so severe and the correlation between crimes is low.

Figure 3 shows the standardized simulated covariate \mathbf{X}_1^* and spatial effects $\boldsymbol{\theta}_1$ and $\boldsymbol{\theta}_2$ for each of the crimes. The first row shows the spatial patterns for Scenario 1 and the second row for Scenario 2. For each of the scenarios a total of $L = 300$ counts data sets are generated. Supplementary material B presents the details about the data generating process of some additional scenarios, Scenarios 3, 4 and 5, and their results.

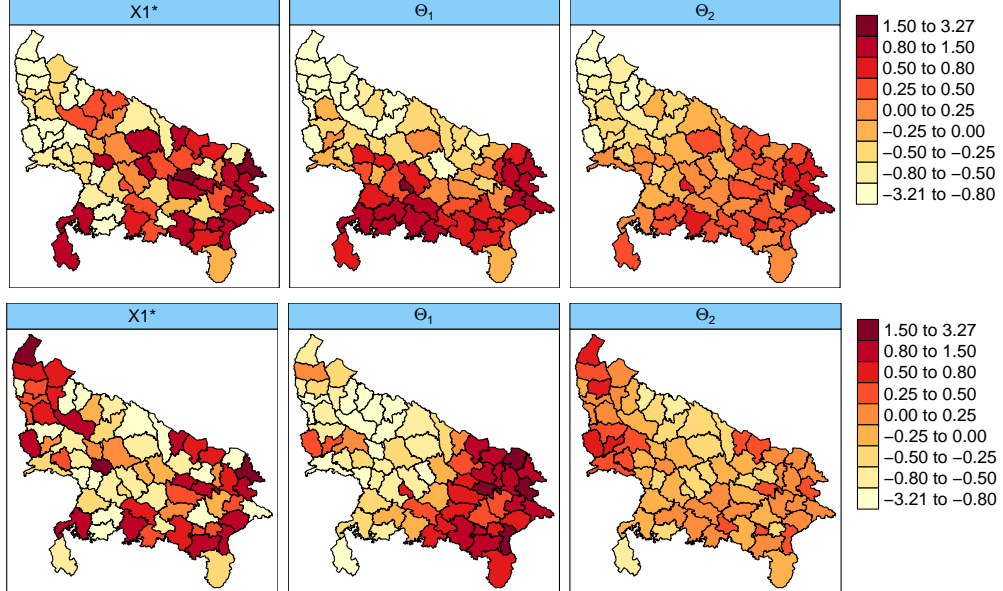


Figure 3: From left to right, standardized simulated covariate \mathbf{X}_1^* , spatial effects $\boldsymbol{\theta}_1$ for crime 1 and spatial effects $\boldsymbol{\theta}_2$ for crime 2 in Simulation Study 2. The top row corresponds to Scenario 1 and the bottom row to Scenario 2.

The simulated data are analysed using the same models as those employed in the real data analysis. All the models are fitted assigning ICAR, PCAR and BYM2 priors to the spatial random effects. The objective is to examine in more detail how the spatial+ method recovers the true fixed effects in different scenarios and if the between-crimes correlation estimates are affected by the method.

6.1 Simulation study 1: Results

The main goal of this simulation study is to evaluate the fixed effect estimates of spatial+ method in multivariate models. Intuitively, the correlation between the unobserved covariates should be captured by the between-crimes covariance matrix, so we will also look at those parameters.

Tables 5 and 6 provide the average over the 300 simulated datasets of the posterior means and posterior standard deviations of the regression coefficients β_1 and β_2 respectively. To visually examine the fixed effect estimates of different models, Figures B.5 and B.6 display boxplots of the posterior means of β_1 and β_2 over the 300 simulated datasets for Scenarios 1 and 2 respectively. In general, the M-Spatial model provides highly biased fixed effects estimates whereas some of the M-models with the spatial+ method recover quite well the true values of the regression coefficients.

The number of large-scale eigenvectors of \mathbf{Q} that should be omitted in \mathbf{Z} and hence assigned to \mathbf{Z}^* (see Equation (3)) depends on the relationship between the observed and unobserved covariates. In the scenarios addressed here, we contemplate correlations of 0.5 and 0.3 (moderate and low) between sex ratio and the unobserved covariate in crime 1 and correlations of 0.7 and 0.5 (high and moderate) in crime 2. Supplementary material A addresses correlations of 0.5, 0.3 and 0.0 (moderate, low and no correlation) between sex ratio and the unobserved covariate \mathbf{X}_2 in crime 1 and correlation of 0.7 (high) between sex ratio and the unobserved covariate \mathbf{X}_3 in crime 2.

Table 5: Posterior means and standard deviations of β_1 based on 300 simulated datasets for Simulation study 1 and Scenarios 1 and 2.

			ICAR		PCAR		BYM2	
	Model	True value	Mean	SD	Mean	SD	Mean	SD
Scenario 1	M-Spatial	-0.1500	-0.2996	0.0674	-0.3162	0.0457	-0.3048	0.0534
	M-SpatPlus64		-0.1869	0.0446	-0.1895	0.0429	-0.1942	0.0433
	M-SpatPlus59		-0.1818	0.0419	-0.1863	0.0407	-0.1932	0.0415
	M-SpatPlus54		-0.1303	0.0407	-0.1315	0.0402	-0.1332	0.0420
	M-SpatPlus49		-0.1141	0.0399	-0.1152	0.0398	-0.1162	0.0419
Scenario 2	M-Spatial	-0.1500	-0.2707	0.0733	-0.2619	0.0477	-0.2590	0.0579
	M-SpatPlus64		-0.1692	0.0481	-0.1710	0.0449	-0.1746	0.0452
	M-SpatPlus59		-0.1648	0.0453	-0.1695	0.0431	-0.1748	0.0440
	M-SpatPlus54		-0.1209	0.0431	-0.1208	0.0422	-0.1211	0.0443
	M-SpatPlus49		-0.1096	0.0419	-0.1110	0.0416	-0.1109	0.0442

Table 6: Posterior means and standard deviations of β_2 based on 300 simulated datasets for Simulation study 1 and Scenarios 1 and 2.

			ICAR		PCAR		BYM2	
	Model	True value	Mean	SD	Mean	SD	Mean	SD
Scenario 1	M-Spatial	-0.2000	-0.3828	0.0596	-0.4140	0.0407	-0.3996	0.0462
	M-SpatPlus64		-0.2258	0.0429	-0.2253	0.0454	-0.2282	0.0438
	M-SpatPlus59		-0.2094	0.0408	-0.2075	0.0432	-0.2143	0.0423
	M-SpatPlus54		-0.1663	0.0396	-0.1655	0.0421	-0.1677	0.0424
	M-SpatPlus49		-0.1412	0.0393	-0.1400	0.0417	-0.1410	0.0426
Scenario 2	M-Spatial	-0.2000	-0.3152	0.0690	-0.3556	0.0443	-0.3403	0.0508
	M-SpatPlus64		-0.1881	0.0465	-0.1885	0.0477	-0.1922	0.0459
	M-SpatPlus59		-0.1779	0.0438	-0.1764	0.0452	-0.1857	0.0443
	M-SpatPlus54		-0.1368	0.0418	-0.1369	0.0439	-0.1403	0.0445
	M-SpatPlus49		-0.1130	0.0411	-0.1116	0.0434	-0.1132	0.0447

In summary, when the correlation between \mathbf{X}_1 and unobserved covariates becomes smaller, lower number of eigenvectors should be omitted in \mathbf{Z} . If too much eigenvectors are excluded from \mathbf{Z} , the M-models with the spatial+ provide biased fixed effects. Nevertheless, in the case of crime 1, a greater number of large-scale eigenvectors should be excluded from \mathbf{Z} compared to crime 2. This discrepancy could be explained because the number of counts for crime 1 is smaller than for crime 2. The M-models with the spatial+ approach provide the same fixed effects estimates irrespective of the prior (ICAR, PCAR or BYM2) given to the spatial random effects. For the M-Spatial model, slight differences are observed in the mean estimates depending on the prior chosen.

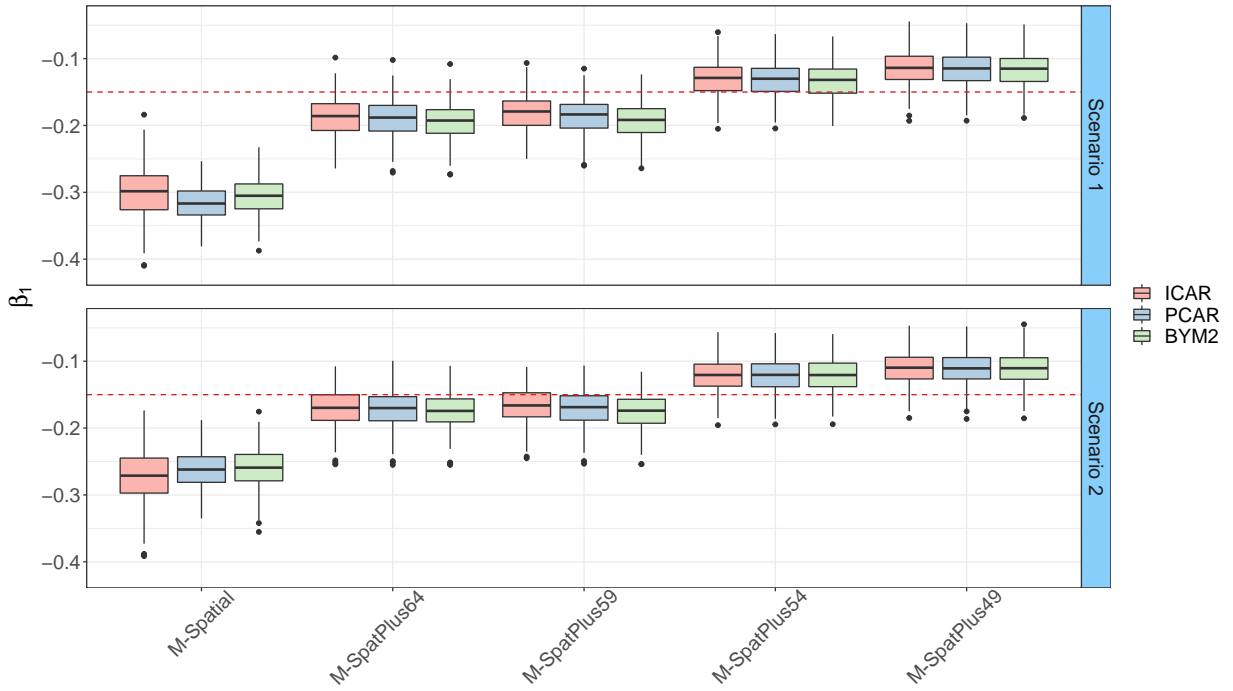


Figure 4: Boxplots of the estimated means of β_1 based on 300 simulated datasets for Simulation Study 1, Scenario 1 (top row) and Scenario 2 (bottom row). Each color represents a different prior given to the columns of Φ , namely, red for ICAR, blue for PCAR and green for BYM2.

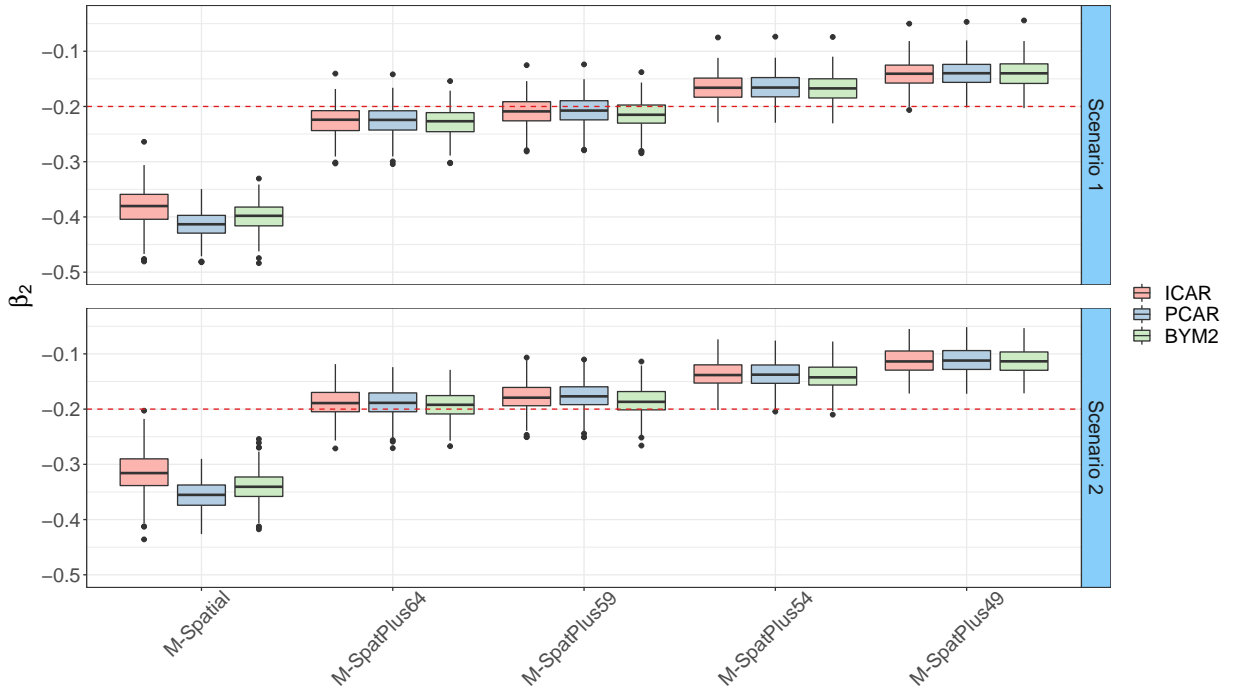


Figure 5: Boxplots of the estimated means of β_2 based on 300 simulated datasets for Simulation Study 1, Scenario 1 (top row) and Scenario 2 (bottom row). Each color represents a different prior given to the columns of Φ , namely, red for ICAR, blue for PCAR and green for BYM2.

Examining Tables 5 and 6 we see that the M-SpatPlus models provide smaller posterior standard deviations than the M-Spatial model. The reduction is about 30%. However, drawing a definitive conclusion regarding whether the posterior standard deviation accurately measures the variability of the fixed effect estimates based on this information is not straightforward. Table A.3 and A.4 in Supplementary material A provide the true simulated standard error ($s.e._{sim}$) and estimated standard

$$\text{error } (s.e._{est}) \text{ for } \beta_1 \text{ and } \beta_2 \text{ computed as } s.e._{sim} = \sqrt{\frac{1}{300} \sum_{l=1}^{300} (\hat{\beta}_j^l - \bar{\beta}_j)^2} \text{ and } s.e._{est} = \frac{1}{300} \sum_{l=1}^{300} sd(\hat{\beta}_j^l)$$

for $j = 1, 2$. Here $\hat{\beta}_j^l$ is the posterior mean of β_j estimated in simulation l and $\bar{\beta}_j$ is the average of all the posterior mean estimates across the simulations. Finally, $sd(\hat{\beta}_j^l)$ is the posterior standard deviation of β_j in simulation l . Overestimation of the posterior standard deviation occurs if the estimated standard error is higher than the simulated standard deviation. In the other way around, the posterior standard deviation of the fixed effect is underestimated if the estimated standard error is lower than the simulated standard deviation. Here, both the M-Spatial and the M-SpatPlus models tend to overestimate the variance of the fixed effects.

To complete the information about fixed effects, Table 7 provides the empirical coverage of credible intervals at 95% nominal value for β_1 and β_2 . In general, the empirical coverages of β_1 and β_2 are relatively low when using the M-Spatial model. This can be attributed to the large bias introduced by the method. On the contrary, the M-models with the spatial+ approach that remove an appropriate number of eigenvectors exhibit credible intervals with certain overcoverage. This could be explained because the spatial+ approach reduces bias but still inflates the variance. If too many eigenvectors are removed, the coverage is poor because the bias increases.

Table 7: Empirical 95% coverage probabilities of the true value of β_1 and β_2 based on 300 simulated datasets for Simulation study 1 and Scenarios 1 and 2.

Model	β_1			β_2		
	ICAR	PCAR	BYM2	ICAR	PCAR	BYM2
Scenario 1	M-Spatial	35.6667	0.0000	5.6667	3.0000	0.0000
	M-SpatPlus64	96.3333	94.6667	93.0000	98.0000	98.6667
	M-SpatPlus59	96.3333	95.3333	93.6667	99.0000	100.0000
	M-SpatPlus54	97.6667	98.3333	100.0000	96.3333	97.3333
	M-SpatPlus49	95.6667	95.6667	96.6667	77.3333	80.3333
Scenario 2	M-Spatial	72.6667	26.6667	53.3333	70.0000	0.6667
	M-SpatPlus64	99.0000	98.6667	98.6667	100.0000	100.0000
	M-SpatPlus59	99.6667	99.0000	98.6667	99.3333	99.6667
	M-SpatPlus54	98.3333	97.6667	99.3333	75.6667	84.0000
	M-SpatPlus49	95.0000	95.3333	97.0000	42.3333	47.0000

Table 8 displays the average over the 300 simulated data sets of the posterior medians and 95% credible intervals of the between crime correlation in each scenario. Here, we contemplate correlations of 0.7 (Scenario 1) and 0.3 (Scenario 2) between the unobserved covariates \mathbf{X}_2 and \mathbf{X}_3 . In both scenarios, the results vary depending on the model and the prior chosen. In general, higher correlations between crimes are estimated when the BYM2 prior is assigned to the spatial random effects. When a high number of large-scale eigenvectors are excluded from the observed covariate, M-SpatPlus exhibits higher correlations between crimes. This probably occurs because the spatial dependence removed from the covariate with spatial+ is represented by the spatial effects. As

a result, the spatial patterns of both crimes may become more similar, potentially leading to an increased correlation between the two crimes. Moreover, the correlation between crimes estimated with the M-models depends on the correlation between \mathbf{X}_2 and \mathbf{X}_3 defined in the data generating model. Overall, the estimated between-crimes correlations are close to the correlations between \mathbf{X}_2 and \mathbf{X}_3 . It is worth noting that the M-models with the spatial+ approach and the BYM2 prior tend to overestimate the correlations. Finally, when the correlation is low, the credible intervals are wider.

Table 8: Posterior medians and 95% credible intervals of estimated correlations between crime 1 and crime 2 based on 300 simulated datasets for Simulation study 1 and Scenarios 1 and 2.

	Model	ICAR			PCAR			BYM2		
		Median	95% CI		Median	95% CI		Median	95% CI	
Scenario 1	M-Spatial	0.7287	0.3607	0.9305	0.6256	0.2464	0.8739	0.5857	0.1678	0.8694
	M-SpatPlus64	0.7277	0.4032	0.9191	0.6313	0.3150	0.8598	0.8099	0.5331	0.9439
	M-SpatPlus59	0.7229	0.3931	0.9178	0.6237	0.3140	0.8541	0.8164	0.5461	0.9459
	M-SpatPlus54	0.7830	0.5067	0.9380	0.6852	0.3879	0.8868	0.8691	0.6472	0.9631
	M-SpatPlus49	0.7958	0.5360	0.9410	0.7045	0.4168	0.8942	0.8808	0.6749	0.9664
Scenario 2	M-Spatial	0.1535	-0.2631	0.5401	0.1710	-0.2115	0.5273	0.2759	-0.2240	0.6615
	M-SpatPlus64	0.2138	-0.1782	0.5729	0.2325	0.0381	0.4566	0.6084	0.2456	0.8345
	M-SpatPlus59	0.1989	-0.1966	0.5643	0.2194	0.0362	0.4368	0.5921	0.2223	0.8228
	M-SpatPlus54	0.3065	-0.0621	0.6327	0.3038	0.0830	0.5458	0.7018	0.3673	0.8864
	M-SpatPlus49	0.3371	-0.0224	0.6506	0.3378	0.0963	0.5970	0.7243	0.4087	0.8919

To conclude the simulation study, we look at model selection criteria and the relative risks estimates. According to Table 9, these criteria do not clearly select any model, though models with the BYM2 prior present slightly lower values, particularly if we compare it with ICAR prior. Table A.8 in Supplementary material A provides MARB and MRRMSE of the relative risks. M-Spatial and M-SpatPlus models perform similarly in terms of the relative risks estimates and differences between spatial priors are negligible.

Table 9: DIC and WAIC based on 300 simulated data sets for Simulation Study 1 and Scenarios 1 and 2.

	Model	ICAR		PCAR		BYM2	
		DIC	WAIC	DIC	WAIC	DIC	WAIC
Scenario 1	M-Spatial	946.0498	952.7725	939.1256	937.2348	934.8325	930.7239
	M-SpatPlus64	944.8425	947.5755	941.3371	937.9480	937.8670	930.4969
	M-SpatPlus59	945.1169	947.9748	941.2409	937.7502	937.9337	930.6553
	M-SpatPlus54	945.8632	947.4914	942.4370	937.5271	940.5496	932.8373
	M-SpatPlus49	946.5776	947.8275	943.0707	937.6770	941.4065	933.3797
Scenario 2	M-Spatial	961.6077	962.9980	953.7916	946.1904	949.2563	939.0299
	M-SpatPlus64	960.3800	958.9302	953.9252	945.8736	950.2834	937.4415
	M-SpatPlus59	960.3221	959.2081	953.7474	946.2881	949.9048	937.1384
	M-SpatPlus54	960.7991	957.1269	954.7606	944.6926	952.5815	938.9499
	M-SpatPlus49	961.0325	956.6160	955.0791	944.1604	953.0834	939.0144

6.2 Simulation study 2: Results

The primary objective of this second simulation study is to evaluate how well the proposed multivariate models estimate the correlations between crimes and the fixed effects. In the data

simulation, the dependence between crimes is introduced by the covariance matrix Σ_b where ρ defines the correlation between the spatial patterns of crime 1 and crime 2. Hence, we will compare the estimated correlations with the true ρ used in the data generating process. Moreover, we will also examine the fixed effect estimates as in Simulation Study 1.

Table 10: Posterior medians and 95% credible intervals of estimated correlations between crime 1 and crime 2 based on 300 simulated datasets for Simulation study 2 and Scenario 1 ($\rho = 0.7$) and Scenario 2 ($\rho = 0.3$).

	Model	ICAR			PCAR			BYM2		
		Median	95% CI		Median	95% CI	Median	95% CI		
Scenario 1 ($\rho = 0.7$)	M-Spatial	0.6991	0.4669	0.8547	0.6825	0.4611	0.8404	0.7328	0.4952	0.8854
	M-SpatPlus64	0.6951	0.4738	0.8456	0.6889	0.4795	0.8359	0.7184	0.4928	0.8664
	M-SpatPlus59	0.6783	0.4499	0.8347	0.6745	0.4624	0.8264	0.7008	0.4718	0.8543
	M-SpatPlus54	0.6954	0.4775	0.8438	0.6883	0.4841	0.8338	0.7177	0.4954	0.8642
	M-SpatPlus49	0.7062	0.4926	0.8516	0.6977	0.4996	0.8379	0.7271	0.5102	0.8698
	M-SpatPlus44	0.7192	0.5137	0.8586	0.7081	0.5116	0.8467	0.7398	0.5326	0.8752
	M-SpatPlus39	0.7221	0.5197	0.8599	0.7086	0.5148	0.8462	0.7454	0.5369	0.8806
Scenario 2 ($\rho = 0.3$)	M-Spatial	0.4529	0.1511	0.6942	0.3180	0.0074	0.6090	0.5037	0.1921	0.7490
	M-SpatPlus64	0.4873	0.1998	0.7148	0.3865	0.1048	0.6429	0.5533	0.2664	0.7764
	M-SpatPlus59	0.5058	0.2339	0.7195	0.4128	0.1378	0.6579	0.5699	0.2971	0.7799
	M-SpatPlus54	0.4969	0.2232	0.7131	0.4042	0.1293	0.6528	0.5596	0.2856	0.7728
	M-SpatPlus49	0.5155	0.2469	0.7254	0.4233	0.1469	0.6687	0.5761	0.3092	0.7808
	M-SpatPlus44	0.5439	0.2913	0.7417	0.4510	0.1761	0.6892	0.6068	0.3498	0.7997
	M-SpatPlus39	0.5588	0.3129	0.7501	0.4629	0.1801	0.7040	0.6226	0.3742	0.8097

Table 10 displays the averages over the 300 simulated data sets of the posterior median and 95% credible intervals of the between-crime correlations in each scenario. Here, the data generating process assumes $\rho = 0.7$ (Scenario 1), $\rho = 0.3$ (Scenario 2), that is, high and low correlations between the spatial patterns of the crimes. For the high correlation scenario, all the M-models effectively capture ρ , but for low correlation, ρ is overestimated. Indeed, in line with the Simulation Study 1 for the low correlation scenario, the estimates of ρ increase in the M-SpatPlus models as more large-scale eigenvectors are removed. Additionally, unlike in Simulation Study 1, the correlation parameter ρ is significant as the credible intervals are not too wide. This is probably because the generating model is the same as the fitted model. Supplementary material B examines a scenario (Scenario 3) in which the data generating model assumes a moderate correlation $\rho = 0.5$ between the spatial patterns. In this case, the estimated correlation coefficient ρ is also overestimated (See Table B.12). In general, the overestimation of ρ is larger with the BYM2 prior than with the ICAR and PCAR priors.

Regarding the fixed effects, Table 11 and Table 12 show the average over the 300 simulated datasets of the posterior means and posterior standard deviations of the regression coefficients β_1 (crime 1) and β_2 (crime 2) in Scenarios 1 and 2 respectively. Figure 6 and 7 provide the boxplots of the posterior means of β_1 and β_2 over the 300 simulated data sets. Looking at these tables and figures, some differences can be observed compared to Simulation Study 1. Here, in the M-SpatPlus models, the number of eigenvectors that must be omitted from the observed covariate to recover the fixed effects does not appear to depend on the linear correlation between \mathbf{X}_1^* and the spatial effects used in the data generating model, but rather on the spatial pattern of the covariate. The covariate and both spatial patterns of Scenario 1 have quite similar structure: the values of the districts in the northwest are low, and as we move to the middle southeast districts, the values gradually increase. Conversely, in Scenario 2 the structures are more complex. The spatial patterns show contrasting directions, and somehow a combination of both spatial patterns can be observed in

Table 11: Posterior means and standard deviations of β_1 based on 300 simulated datasets for Simulation study 2 and Scenarios 1 and 2.

	Model	True value	ICAR		PCAR		BYM2	
			Mean	SD	Mean	SD	Mean	SD
Scenario 1	M-Spatial	0.1500	0.2701	0.0815	0.2766	0.0837	0.2760	0.0846
	M-SpatPlus64		0.1878	0.0612	0.1871	0.0619	0.1895	0.0630
	M-SpatPlus59		0.1914	0.0585	0.1915	0.0593	0.1961	0.0605
	M-SpatPlus54		0.1709	0.0580	0.1705	0.0587	0.1731	0.0599
	M-SpatPlus49		0.1580	0.0563	0.1579	0.0571	0.1600	0.0584
	M-SpatPlus44		0.1405	0.0547	0.1407	0.0555	0.1425	0.0574
Scenario 2	M-SpatPlus39		0.1260	0.0517	0.1260	0.0526	0.1289	0.0549
	M-Spatial	0.1500	0.2688	0.0685	0.2726	0.0712	0.2733	0.0708
	M-SpatPlus64		0.2406	0.0656	0.2400	0.0681	0.2407	0.0675
	M-SpatPlus59		0.2160	0.0640	0.2140	0.0665	0.2140	0.0656
	M-SpatPlus54		0.2173	0.0625	0.2157	0.0650	0.2164	0.0642
	M-SpatPlus49		0.1996	0.0612	0.1982	0.0636	0.1985	0.0631
	M-SpatPlus44		0.1700	0.0599	0.1685	0.0624	0.1683	0.0624
	M-SpatPlus39		0.1454	0.0567	0.1445	0.0593	0.1441	0.0599

Table 12: Posterior means and standard deviations of β_2 based on 300 simulated datasets for Simulation study 2 and Scenarios 1 and 2.

	Model	True value	ICAR		PCAR		BYM2	
			Mean	SD	Mean	SD	Mean	SD
Scenario 1	M-Spatial	0.2000	0.3018	0.0476	0.3284	0.0519	0.3179	0.0501
	M-SpatPlus64		0.2055	0.0380	0.2051	0.0404	0.2069	0.0398
	M-SpatPlus59		0.1938	0.0370	0.1935	0.0393	0.1947	0.0388
	M-SpatPlus54		0.1829	0.0367	0.1829	0.0390	0.1830	0.0385
	M-SpatPlus49		0.1741	0.0355	0.1739	0.0378	0.1745	0.0374
	M-SpatPlus44		0.1605	0.0353	0.1599	0.0375	0.1613	0.0375
Scenario 2	M-SpatPlus39		0.1304	0.0341	0.1302	0.0364	0.1312	0.0367
	M-Spatial	0.2000	0.2876	0.0381	0.2914	0.0393	0.2997	0.0399
	M-SpatPlus64		0.2674	0.0371	0.2694	0.0382	0.2771	0.0392
	M-SpatPlus59		0.2394	0.0380	0.2403	0.0389	0.2423	0.0401
	M-SpatPlus54		0.2314	0.0374	0.2323	0.0383	0.2337	0.0395
	M-SpatPlus49		0.2189	0.0368	0.2190	0.0376	0.2213	0.0389
	M-SpatPlus44		0.1876	0.0378	0.1880	0.0384	0.1905	0.0404
	M-SpatPlus39		0.1454	0.0373	0.1458	0.0379	0.1472	0.0404

\mathbf{X}_1^* . In the high correlation scenario (Scenario 1), removing 20 large-scale eigenvectors from the covariate seems enough to recover β_1 (see Table 11) and between 5 to 15 eigenvectors for β_2 (see Table 12). For crime 2 less eigenvectors are enough probably because the number of simulated counts is larger. In contrast, when examining the low correlation scenario (Scenario 2), the removal of 20 large-scale eigenvectors in the M-SpatPlus models leads to an overestimation of the fixed effects, particularly for crime 1 (see Table 11). To address this issue, we have fitted the M-SpatPlus model removing more eigenvectors from the covariate. Specifically, we have remove 25 and 30 large-scale eigenvectors (M-SpatPlus44 and M-SpatPlus39 respectively in the tables). Interestingly, when 30 large-scale eigenvectors were removed, the M-SpatPlus estimates of β_1 are satisfactory. There are no considerable differences between the ICAR, PCAR and BYM2 priors in terms of the fixed effect estimates.

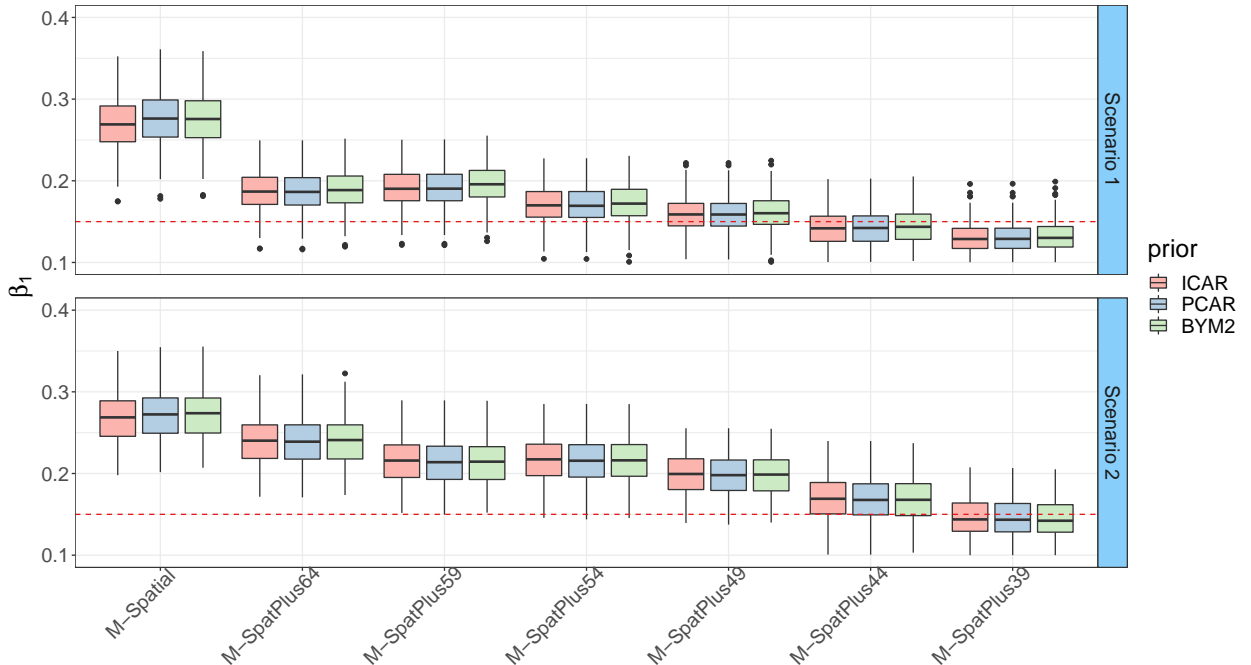


Figure 6: Boxplots of the estimated means of β_1 based on 300 simulated datasets for Simulation Study 2, Scenario 1 (top row) and Scenario 2 (bottom row). Each color represents a different prior given to the columns of Φ , namely, red for ICAR, blue for PCAR and green for BYM2.

Similarly to Simulation Study 1, we have compare the true simulated standard error ($s.e._{sim}$) and the estimated standard error ($s.e._{est}$) for β_1 and β_2 (see Tables B.15 and B.16 of the Supplementary material B) and we provide the empirical coverage of credible intervals at 95% nominal value for β_1 and β_2 (Table 13). The overestimation of the standard deviations of β_1 is quite apparent (see Table B.15). The estimated standard deviation is approximately three times the simulated estandard error. This overestimation is reflected in the 95% coverage probabilities of M-SpatPlus, where nearly all the methods lead to an overcoverage. The reason is that the M-SpatialPlus models reduce bias, but still the variance seems inflated, hence the excess of coverage. In the case of β_2 the overestimation of the standard deviations is lower (see Table B.16) and more reasonable 95% coverage probabilities are obtained for the M-SpatPlus models. As in Simulation Study 1, the empirical coverage of β_1 and β_2 with usual multivariate M-Spatial model is low because the overestimation of the standard deviation does not compensate for the large bias.

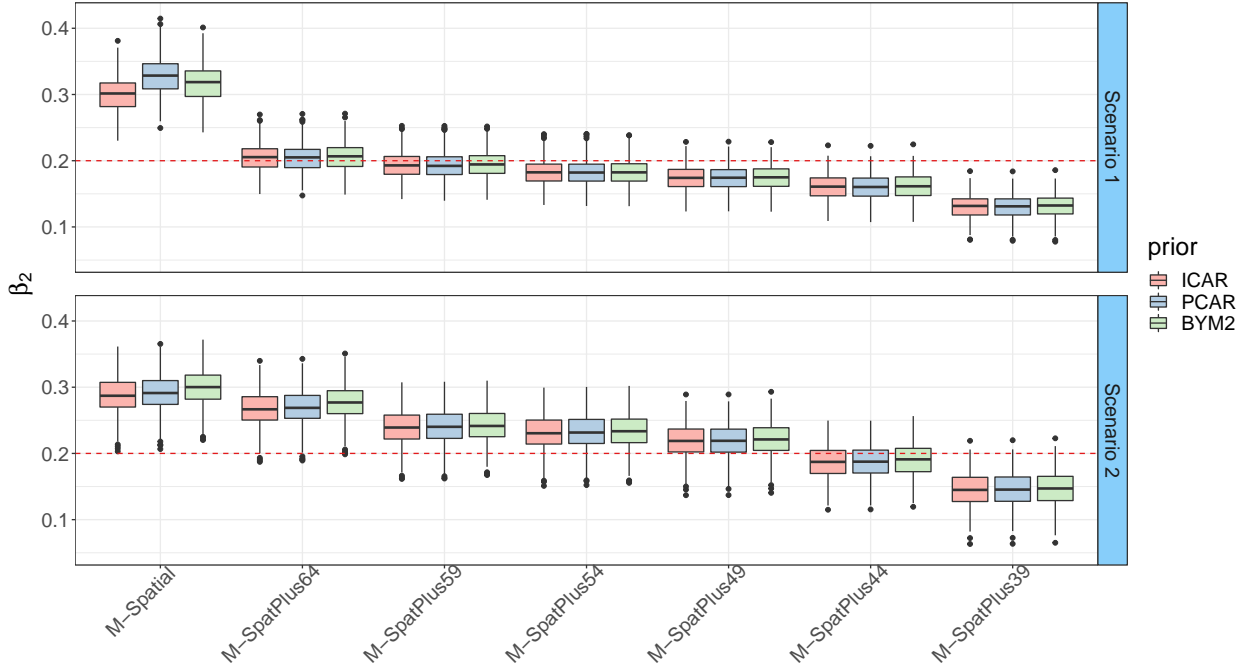


Figure 7: Boxplots of the estimated means of β_2 based on 300 simulated datasets for Simulation Study 2, Scenario 1 (top row) and Scenario 2 (bottom row). Each color represents a different prior given to the columns of Φ , namely, red for ICAR, blue for PCAR and green for BYM2.

To finish, we examine model selection criteria and MARB and MRRMSE of the relative risks estimates. Table 14 provides the DIC and WAIC for Scenarios 1 and 2. Again, model selection criteria do not effectively differentiate between the models and spatial priors. Table B.19 provides MARB and MRRMSE of the relative risks. All the M-models have similar bias and error concerning the relative risks estimates.

Table 13: Empirical 95% coverage probabilities of the true value of β_1 and β_2 based on 300 simulated datasets for Simulation study 2 and Scenarios 1 and 2.

	Model	β_1			β_2		
		ICAR	PCAR	BYM2	ICAR	PCAR	BYM2
Scenario 1	M-Spatial	86.0000	84.6667	85.0000	40.3333	19.6667	25.3333
	M-SpatPlus64	100.0000	100.0000	100.0000	100.0000	100.0000	100.0000
	M-SpatPlus59	100.0000	100.0000	100.0000	100.0000	100.0000	100.0000
	M-SpatPlus54	100.0000	100.0000	100.0000	100.0000	100.0000	100.0000
	M-SpatPlus49	100.0000	100.0000	100.0000	99.3333	99.3333	99.3333
	M-SpatPlus44	100.0000	100.0000	100.0000	92.3333	95.3333	95.6667
Scenario 2	M-SpatPlus39	100.0000	100.0000	100.0000	47.0000	57.6667	61.0000
	M-Spatial	70.0000	70.6667	69.3333	31.6667	28.0000	20.6667
	M-SpatPlus64	91.0000	92.6667	92.6667	57.3333	56.6667	51.0000
	M-SpatPlus59	98.6667	99.0000	99.0000	91.6667	91.3333	92.3333
	M-SpatPlus54	98.3333	99.0000	99.0000	95.0000	95.0000	95.3333
	M-SpatPlus49	100.0000	100.0000	100.0000	98.3333	98.6667	98.6667
	M-SpatPlus44	100.0000	100.0000	100.0000	99.0000	99.3333	99.6667
	M-SpatPlus39	100.0000	100.0000	100.0000	76.3333	77.6667	87.0000

Table 14: DIC and WAIC based on 300 simulated data sets for Simulation Study 2 and Scenarios 1 and 2.

	Model	ICAR		PCAR		BYM2	
		DIC	WAIC	DIC	WAIC	DIC	WAIC
Scenario 1	M-Spatial	966.1754	951.4779	967.5752	950.1012	967.0064	948.7606
	M-SpatPlus64	966.8528	949.4872	967.9400	948.4048	967.9372	947.5738
	M-SpatPlus59	967.6719	950.0178	968.8122	949.0177	968.8697	948.4177
	M-SpatPlus54	967.8177	949.9382	968.9508	948.8622	969.1185	948.4952
	M-SpatPlus49	968.4432	950.9564	969.5225	949.7588	969.7227	949.5140
	M-SpatPlus44	969.1746	951.9225	970.1753	950.5237	970.4424	950.4116
Scenario 2	M-SpatPlus39	971.8599	955.0197	972.7043	953.2348	973.0639	953.3253
	M-Spatial	969.8757	952.8217	970.7773	949.9615	970.5796	949.5215
	M-SpatPlus64	969.9933	952.1133	970.6760	949.0728	970.6719	948.8739
	M-SpatPlus59	971.2157	951.1453	972.0652	948.4785	972.2841	948.9999
	M-SpatPlus54	971.8931	951.8211	972.7483	949.2491	973.0684	949.9883
	M-SpatPlus49	973.0603	953.3003	973.8526	950.6847	974.2231	951.4681
	M-SpatPlus44	975.0822	954.8057	975.8658	952.0949	976.2864	952.9832
	M-SpatPlus39	978.8893	959.4039	979.5481	956.4251	979.9821	957.2993

7 Discussion

The inclusion of the covariates in spatial models, whether they are univariate or multivariate, faces the well known problem of spatial confounding, that is, the impossibility of disentangling the fixed effects and the spatial random effects. A correct estimation of the fixed effects is crucial to gain knowledge about complex diseases like cancer or intricate socio-demographic phenomena, such as crimes against women in India.

To deal with spatial confounding, different methods have been proposed in the literature, but we focus on the spatial+ approach as it has proven to work well at least in univariate spatial models. In this paper we propose a modified and simpler version of the method that can be fitted in one step unlike the original proposal that fits two models. In our proposal the covariate is expressed as a linear combination of the eigenvectors of the spatial precision matrix, and the spatial dependence is removed discarding part of the linear combination that corresponds to a certain number of large-scale eigenvectors. With this modified spatial+ approach we avoid fitting a model to the covariate and we directly consider a “spatially decorrelated” version of the covariate. The method can be used in univariate as well as in multivariate models, but in this work we focus on the latter. The method is simple and flexible and allows a different “spatial decorrelation” of the covariates depending of the responses.

To illustrate the proposal, two crimes against women, namely rapes and dowry deaths, are analysed jointly in the 70 districts of Uttar Pradesh in 2011. In particular, we have focused on the linear association between the covariate sex ratio and the crimes. All the multivariate models indicate that there is no significant linear association between sex ratio and rapes, whereas for dowry deaths the strength of the association depends on the number of removed eigenvectors from the covariate. Additionally, all the models estimate a rather low positive correlation between rapes and dowry deaths that is on the verge of statistical significance. Our proposal requires consideration about the number of eigenvectors to remove from the linear combination of the covariate. To provide some guidelines, we have conducted two simulation studies. In Simulation Study 1, spatial confounding is induced including two covariates in the data generating model for each crime. Namely, the sex ratio (\mathbf{X}_1) for both crimes, \mathbf{X}_2 for crime 1 and \mathbf{X}_3 for crime 2. The covariates \mathbf{X}_2 and \mathbf{X}_3 play the role of unobserved covariates (they are replaced by spatial random effects in the fit) and are correlated, hence they induce dependence between crimes. In Simulation study 2, we have generated the spatial effects $\boldsymbol{\theta}_1$ and $\boldsymbol{\theta}_2$ for crimes 1 and 2 respectively from a multivariate ICAR prior with fixed correlation parameter. These spatial effects are responsible of causing correlation between crimes. Then, the observed covariate \mathbf{X}_1^* , is simulated to be correlated with both the spatial effects, $\boldsymbol{\theta}_1$ and $\boldsymbol{\theta}_2$, and different scenarios are simulated depending on the correlations between the covariates and the spatial effects. Overall, the findings of the simulation studies are interesting. The M-models with the original covariate without the spatial+ method do not recover the true fixed effects in any of the simulated scenarios. This is particularly striking in Scenario 2 where the multivariate ICAR is the data generating model. On the contrary, M-models with the spatial+ method provide fairly unbiased estimates and the estimates do not depend on the prior given to the spatial random effects. The key lies in determining beforehand the amount of spatial dependence that we should remove from the covariate. In Simulation Study 1, where the observed covariate (sex ratio) has a clear and gradual spatial pattern, the greater the correlation between the observed and the unobserved covariates, the larger the number of eigenvectors to remove. To be more specific, we should remove between 7% and 20% of the eigenvectors corresponding to the lowest eigenvalues. It is worth noting that in crime 1 we have to remove more eigenvectors than in crime 2, probably because the number of counts is smaller.

In Simulation study 2, results are revealing. It seems that the number of eigenvectors to remove depends more on the spatial dependence of the observed covariate than on the correlation between the observed and unobserved parts of the model. In scenario 1, where the spatial pattern of the simulated observed covariate is more or less smooth and the correlation with the unobserved part is moderate-high, we need to remove about 28% of the eigenvectors in crime 1 and between 7% and 14% of the eigenvectors for crime 2. In scenario 2, where the spatial pattern of the covariate is not so smooth and the correlation with the unobserved part is low-moderate, we need to remove between 35% and 43% of the eigenvectors. As in Simulation Study 1, we need to remove more eigenvectors in crime 1 than in crime 2.

To sum up, if the spatial pattern of the observed covariate is smooth, removing 7% to 20% of the eigenvectors should be a good choice. If the spatial pattern of the covariate is not so smooth, then we should remove 35% to 43% eigenvectors. We find these guidelines useful as they depend on the observed covariate rather than on the unobserved ones.

In terms of the between-crime correlation estimates, all models recover quite well high correlations, though low-moderate correlations might be overestimated. Moreover, the overestimation is larger if we remove more eigenvectors than needed. Additionally, the overestimation is larger with the BYM2 spatial prior.

The multivariate models employing the spatial+ approach address bias in the estimates of fixed effects. However, there seems to be an issue with inflated standard errors, leading to a significant overcoverage of the credible intervals. Further research is necessary to adequately adjust the standard errors. Additionally, model selection criteria such as DIC or WAIC do not differentiate between the models. This is somewhat expected, considering that the spatial+ approach can be seen as a reparameterized spatial model.

Finally, it is worth noting that the proposed modified spatial+ approach is valid for univariate and multivariate models. In general we do not expect big differences in the estimation of the fixed effects in univariate and multivariate models if a true relationship between the responses and the covariate exists. However, we think that in complex phenomena such as crimes against women (or cancer, where risk factors only explain a small percentage of cases) multivariate models are more convenient to deal with the problem as a whole and not with each part individually.

Acknowledgements

This work has been supported by Project PID2020-113125RB-I00/MCIN/AEI/10.13039/501100011033.

References

- Adin, A., Goicoa, T., Hodges, J. S., Schnell, P. M., & Ugarte, M. D. (2023). Alleviating confounding in spatio-temporal areal models with an application on crimes against women in India. *Statistical Modelling*, 23(1), 9–30. <https://doi.org/10.1177/1471082X211015452>
- Banerjee, S., Carlin, B. P., & Gelfand, A. E. (2015). *Hierarchical Modelling and Analysis for Spatial Data, Second Edition*. Chapman & Hall, Boca Raton.
- Besag, J. (1974). Spatial interaction and the statistical analysis of lattice systems (with discussion). *Journal of the Royal Statistical Society: Series B (Statistical Methodology)*, 36, 192–236. <https://doi.org/10.1111/j.2517-6161.1974.tb00999.x>
- Botella-Rocamora, P., Martinez-Beneito, M., & Banerjee, S. (2015). A unifying modeling framework for highly multivariate disease mapping. *Statistics in Medicine*, 34(9), 1548–1559. <https://doi.org/10.1002/sim.6423>
- Congdon, P. (2013). Assessing the impact of socioeconomic variables on small area variations in suicide outcomes in england. *International Journal of Environmental Research and Public Health*, 10(1), 158–177. <https://doi.org/10.3390/ijerph10010158>
- Dupont, E., Wood, S. N., & Augustin, N. H. (2022). Spatial+: A novel approach to spatial confounding. *Biometrics*, n/a(n/a), 1–12. <https://doi.org/10.1111/biom.13656>
- Gilbert, B., Datta, A., & Ogburn, E. (2022). Approaches to spatial confounding in geostatistics. *arXiv:2112.14946v2*. <https://doi.org/10.48550/arXiv.2112.14946>
- Goicoa, T., Adin, A., Ugarte, M. D., & Hodges, J. S. (2018). In spatio-temporal disease mapping models, identifiability constraints affect PQL and INLA results. *Stochastic Environmental Research and Risk Assessment*, 32(3), 749–770. <https://doi.org/10.1007/s00477-017-1405-0>
- Guan, Y., Page, G. L., Reich, B. J., Ventrucci, M., & Yang, S. (2022). Spectral adjustment for spatial confounding. *Biometrika*. <https://doi.org/10.1093/biomet/asac069>
- Hanks, E. M., Schliep, E. M., Hooten, M. B., & Hoeting, J. A. (2015). Restricted spatial regression in practice: geostatistical models, confounding, and robustness under model misspecification. *Environmetrics*, 26(4), 243–254. <https://doi.org/10.1002/env.2331>
- Harville, D. A. (2008). *Matrix Algebra from a Statistician's Perspective*. Springer, New York.
- Hodges, J. S. & Reich, B. J. (2010). Adding spatially-correlated errors can mess up the fixed effect you love. *The American Statistician*, 64(4), 325–334. <https://doi.org/10.1198/tast.2010.10052>
- Hughes, J. & Haran, M. (2013). Dimension reduction and alleviation of confounding for spatial generalized linear mixed models. *Journal of the Royal Statistical Society: Series B (Statistical Methodology)*, 75(1), 139–159. <https://doi.org/10.1111/j.1467-9868.2012.01041.x>
- Jin, X., Banerjee, S., & Carlin, B. P. (2007). Order-free co-regionalized areal data models with application to multiple-disease mapping. *Journal of the Royal Statistical Society: Series B (Statistical Methodology)*, 69(5), 817–838. <https://doi.org/10.1111/j.1467-9868.2007.00612.x>
- Khan, K. & Calder, C. A. (2022). Restricted spatial regression methods: implications for inference. *Journal of the American Statistical Association*, 117(537), 482–494. <https://doi.org/10.1080/01621459.2020.1788949>

- Lindgren, F. & Rue, H. (2015). Bayesian spatial modelling with r-inla. *Journal of Statistical Software*, 63(19), 1–25. <https://doi.org/10.18637/jss.v063.i19>
- MacNab, Y. C. (2018). Some recent work on multivariate Gaussian Markov random fields. *Test*, 27(3), 497–541. <https://doi.org/10.1007/s11749-018-0605-3>
- Marques, I., Kneib, T., & Klein, M. (2022). Mitigating spatial confounding by explicitly correlating gaussian random fields. *Environmetrics*, 33(5), e2727. <https://doi.org/10.1002/env.2727>
- Martinez-Beneito, M. A. (2013). A general modelling framework for multivariate disease mapping. *Biometrika*, 100(3), 539–553. <https://doi.org/10.1093/biomet/ast023>
- Martínez-Beneito, M. A. & Botella-Rocamora, P. (2019). *Hierarchical Modelling and Analysis for Spatial Data, Second Edition*. Chapman & Hall, Boca Raton.
- Mukherjee, C., Rustagi, P., & Krishnaji, N. (2001). Crimes against women in India: Analysis of official statistics. *Economic and Political Weekly*, 36(43), 4070–4080.
- Page, G. L., Liu, Y., He, Z., & Sun, D. (2017). Estimation and prediction in the presence of spatial confounding for spatial linear models. *Scandinavian Journal of Statistics*, 44(3), 780–797. <https://doi.org/10.1111/sjos.12275>
- Peña, V. & Irie, K. (2022). On the Relationship between Uhlig Extended and beta-Bartlett Processes. *Journal of Time Series Analysis*, 43(1), 147–153. <https://doi.org/10.1111/jtsa.12595>
- Prates, M. O., Dey, D. K., Willig, M. R., & Yan, J. (2015). Transformed gaussian markov random fields and spatial modeling of species abundance. *Spatial Statistics*, 14(PC), 382–399. <https://doi.org/10.1016/j.spasta.2015.07.004>
- Reich, B. J., Hodges, J. S., & Zadnik, V. (2006). Effects of residual smoothing on the posterior of the fixed effects in disease-mapping models. *Biometrics*, 62(4), 1197–1206. <https://doi.org/10.1111/j.1541-0420.2006.00617.x>
- Riebler, A., Sørbye, S. H., Simpson, D., & Rue, H. (2016). An intuitive bayesian spatial model for disease mapping that accounts for scaling. *Statistical Methods in Medical Research*, 25(4), 1145–1165. <https://doi.org/10.1177/0962280216660421>
- Rue, H., Martino, S., & Chopin, N. (2009). Approximate bayesian inference for latent gaussian models by using integrated nested laplace approximations. *Journal of the Royal Statistical Society: Series B (Statistical Methodology)*, 71(2), 319–392. <https://doi.org/10.1111/j.1467-9868.2008.00700.x>
- Urdangarin, A., Goicoa, T., & Ugarte, M. D. (2023). Evaluating recent methods to overcome spatial confounding. *Revista Complutense Madrid*, 36, 333–360. <https://doi.org/10.1007/s13163-022-00449-8>
- Vicente, G., Adin, A., Goicoa, T., & Ugarte, M. D. (2023a). High-dimensional order-free multivariate spatial disease mapping. *Statistics and Computing (in press)*. <https://doi.org/10.48550/arXiv.2210.14849>
- Vicente, G., Goicoa, T., Fernandez-Rasines, P., & Ugarte, M. D. (2020a). Crime Against Women in India: Unveiling Spatial Patterns and Temporal Trends of Dowry Deaths in the Districts of Uttar Pradesh. *Journal of the Royal Statistical Society Series A: Statistics in Society*, 183(2), 655–679. <https://doi.org/10.1111/rssa.12545>

- Vicente, G., Goicoa, T., Puranik, A., & Ugarte, M. D. (2018). Small area estimation of gender-based violence: rape incidence risks in Uttar Pradesh, India. *Statistics and Applications*, 16(1), 71–90.
- Vicente, G., Goicoa, T., & Ugarte, M. D. (2020b). Bayesian inference in multivariate spatio-temporal areal models using INLA: analysis of gender-based violence in small areas. *Stochastic Environmental Research and Risk Assessment*, 34, 1421–1440. <https://doi.org/10.1007/s00477-020-01808-x>
- Vicente, G., Goicoa, T., & Ugarte, M. D. (2023b). Multivariate Bayesian spatio-temporal P-spline models to analyze crimes against women. *Biostatistics*, 24(3), 562–584. <https://doi.org/10.1093/biostatistics/kxab042>

A Supplementary material: Simulation study 1

This section includes some additional scenarios to complement the analysis of Simulation study 1. The data is generated following the generating models (11)-(12) with $\boldsymbol{\alpha} = (\alpha_1, \alpha_2)' = (-0.12, -0.03)', \boldsymbol{\beta} = (\beta_1, \beta_2)' = (-0.15, -0.20)', \boldsymbol{\beta}^* = (\beta_1^*, \beta_2^*)' = (-0.30, -0.30)'$ and \mathbf{X}_1 is the standardized sex ratio covariate. Below we define the correlations between \mathbf{X}_1 , \mathbf{X}_2 and \mathbf{X}_3 chosen in each scenario:

- **Scenario 3:** $\text{cor}(\mathbf{X}_1, \mathbf{X}_2) = 0.5$, $\text{cor}(\mathbf{X}_1, \mathbf{X}_3) = 0.7$ and $\text{cor}(\mathbf{X}_2, \mathbf{X}_3) = 0.5$ are chosen. This is similar to Scenario 1 but choosing lower correlation between \mathbf{X}_2 and \mathbf{X}_3 .
- **Scenario 4:** $\text{cor}(\mathbf{X}_1, \mathbf{X}_2) = 0.3$, $\text{cor}(\mathbf{X}_1, \mathbf{X}_3) = 0.7$ and $\text{cor}(\mathbf{X}_2, \mathbf{X}_3) = 0.3$ are chosen.
- **Scenario 5:** $\text{cor}(\mathbf{X}_1, \mathbf{X}_2) = 0.0$, $\text{cor}(\mathbf{X}_1, \mathbf{X}_3) = 0.7$ and $\text{cor}(\mathbf{X}_2, \mathbf{X}_3) = 0.7$ are chosen.
- **Scenario 6:** $\text{cor}(\mathbf{X}_1, \mathbf{X}_2) = 0.0$, $\text{cor}(\mathbf{X}_1, \mathbf{X}_3) = 0.7$ and $\text{cor}(\mathbf{X}_2, \mathbf{X}_3) = 0.3$ are chosen.

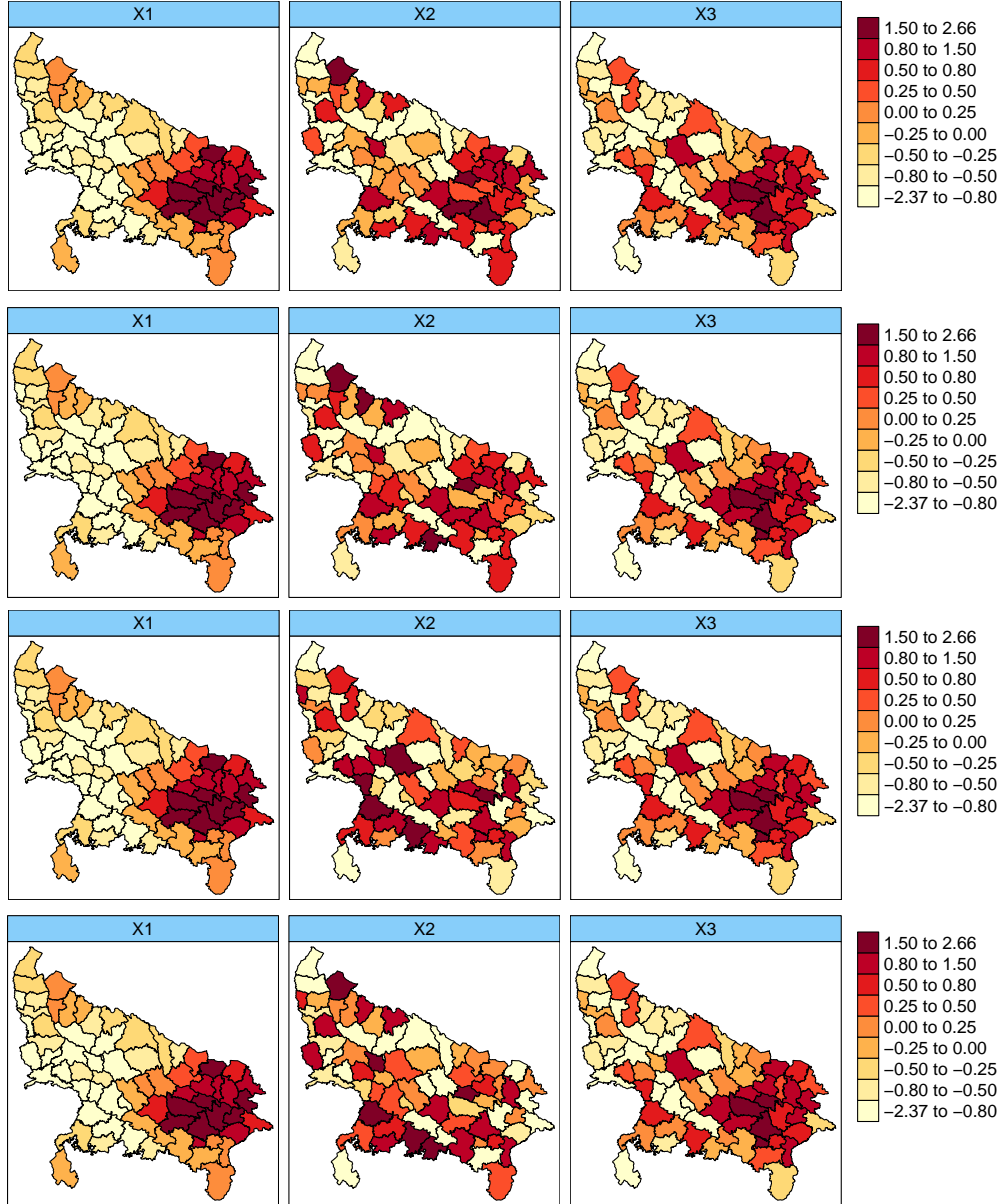


Figure A.1: From left to right, standardized sex ratio covariate in 2011, standardized simulated covariate \mathbf{X}_2 and standardized simulated covariate \mathbf{X}_3 in Simulation Study 1. The first row corresponds to Scenario 3, the second to Scenario 4, the third to Scenario 5 and the last row to Scenario 6.

Table A.1: Posterior means and standard deviations of β_1 based on 300 simulated datasets for Simulation study 1 and Scenarios 3, 4, 5 and 6.

	Model	True value	ICAR		PCAR		BYM2	
			Mean	SD	Mean	SD	Mean	SD
Scenario 3	M-Spatial	-0.1500	-0.3207	0.0684	-0.3169	0.0457	-0.3130	0.0552
	M-SpatPlus64		-0.1988	0.0456	-0.2002	0.0423	-0.2034	0.0432
	M-SpatPlus59		-0.1915	0.0430	-0.1951	0.0406	-0.1995	0.0417
	M-SpatPlus54		-0.1432	0.0416	-0.1434	0.0403	-0.1439	0.0422
	M-SpatPlus49		-0.1288	0.0407	-0.1297	0.0399	-0.1301	0.0421
Scenario 4	M-Spatial	-0.1500	-0.2721	0.0734	-0.2604	0.0476	-0.2596	0.0583
	M-SpatPlus64		-0.1700	0.0482	-0.1715	0.0438	-0.1742	0.0446
	M-SpatPlus59		-0.1653	0.0454	-0.1694	0.0418	-0.1740	0.0432
	M-SpatPlus54		-0.1225	0.0430	-0.1223	0.0407	-0.1222	0.0429
	M-SpatPlus49		-0.1117	0.0418	-0.1126	0.0401	-0.1125	0.0427
Scenario 5	M-Spatial	-0.1500	-0.1067	0.0773	-0.1598	0.0487	-0.1361	0.0567
	M-SpatPlus64		-0.0657	0.0489	-0.0711	0.0488	-0.0772	0.0463
	M-SpatPlus59		-0.0681	0.0461	-0.0742	0.0464	-0.0853	0.0448
	M-SpatPlus54		-0.0386	0.0421	-0.0408	0.0423	-0.0447	0.0433
	M-SpatPlus49		-0.0255	0.0407	-0.0265	0.0408	-0.0280	0.0428
Scenario 6	M-Spatial	-0.1500	-0.1630	0.0737	-0.1711	0.0482	-0.1614	0.0580
	M-SpatPlus64		-0.1046	0.0476	-0.1091	0.0445	-0.1130	0.0453
	M-SpatPlus59		-0.1078	0.0447	-0.1165	0.0422	-0.1232	0.0437
	M-SpatPlus54		-0.0697	0.0417	-0.0711	0.0401	-0.0725	0.0426
	M-SpatPlus49		-0.0609	0.0404	-0.0624	0.0390	-0.0630	0.0421

Table A.2: Posterior means and standard deviations of β_2 based on 300 simulated datasets for Simulation study 1 and Scenarios 3, 4, 5 and 6.

		ICAR		PCAR		BYM2		
	Model	True value	Mean	SD	Mean	SD	Mean	SD
Scenario 3	M-Spatial	-0.2000	-0.3863	0.0593	-0.4138	0.0401	-0.4029	0.0454
	M-SpatPlus64		-0.2299	0.0424	-0.2290	0.0442	-0.2309	0.0435
	M-SpatPlus59		-0.2137	0.0403	-0.2112	0.0421	-0.2162	0.0420
	M-SpatPlus54		-0.1693	0.0392	-0.1687	0.0417	-0.1706	0.0422
	M-SpatPlus49		-0.1446	0.0389	-0.1433	0.0414	-0.1442	0.0424
Scenario 4	M-Spatial	-0.2000	-0.3819	0.0597	-0.4113	0.0403	-0.4001	0.0453
	M-SpatPlus64		-0.2272	0.0426	-0.2267	0.0452	-0.2287	0.0440
	M-SpatPlus59		-0.2121	0.0405	-0.2101	0.0430	-0.2155	0.0425
	M-SpatPlus54		-0.1669	0.0394	-0.1664	0.0423	-0.1685	0.0432
	M-SpatPlus49		-0.1419	0.0391	-0.1405	0.0420	-0.1415	0.0434
Scenario 5	M-Spatial	-0.2000	-0.3730	0.0607	-0.4119	0.0402	-0.3939	0.0455
	M-SpatPlus64		-0.2206	0.0454	-0.2240	0.0477	-0.2282	0.0440
	M-SpatPlus59		-0.2033	0.0430	-0.2066	0.0456	-0.2156	0.0426
	M-SpatPlus54		-0.1614	0.0415	-0.1618	0.0443	-0.1660	0.0437
	M-SpatPlus49		-0.1360	0.0411	-0.1353	0.0439	-0.1372	0.0443
Scenario 6	M-Spatial	-0.2000	-0.3818	0.0590	-0.4128	0.0401	-0.4005	0.0453
	M-SpatPlus64		-0.2253	0.0428	-0.2259	0.0461	-0.2285	0.0437
	M-SpatPlus59		-0.2089	0.0407	-0.2082	0.0438	-0.2150	0.0423
	M-SpatPlus54		-0.1655	0.0396	-0.1650	0.0432	-0.1677	0.0433
	M-SpatPlus49		-0.1394	0.0393	-0.1382	0.0430	-0.1394	0.0438

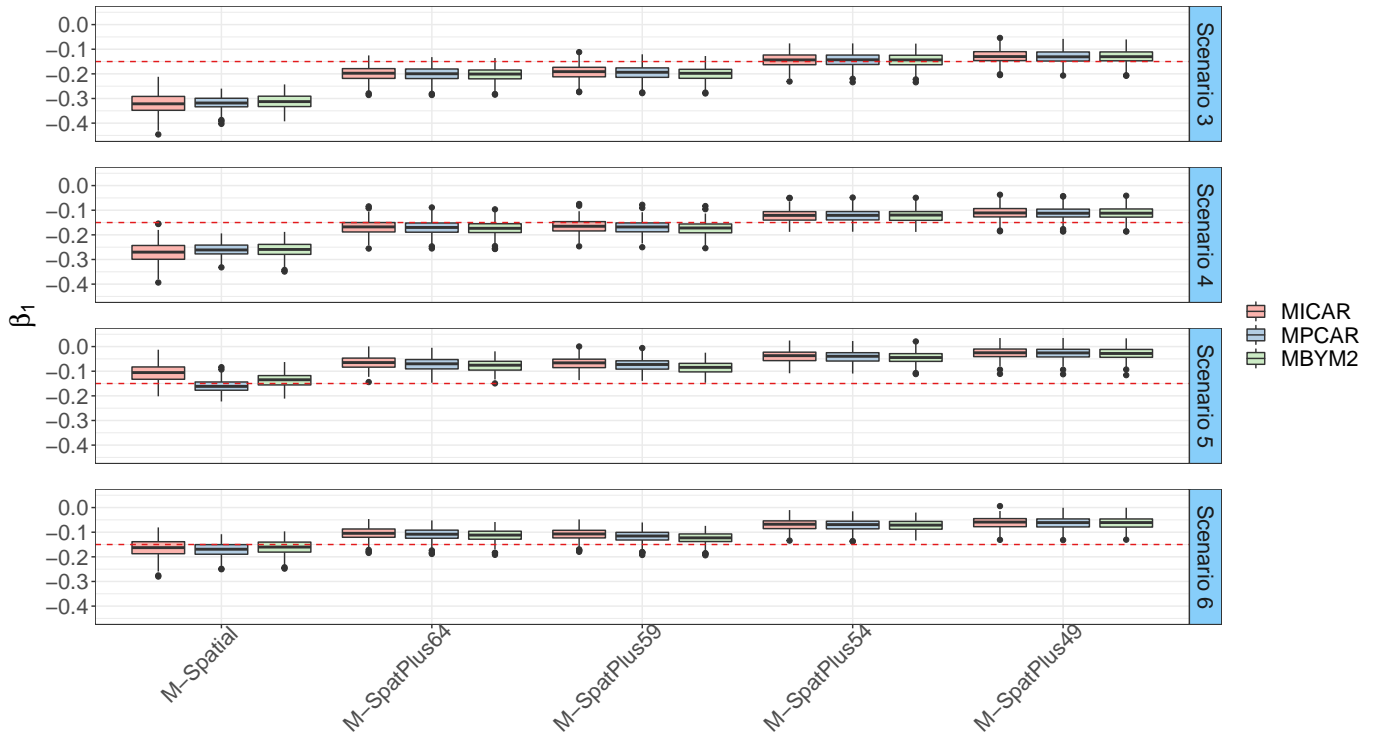


Figure A.2: Boxplots of the estimated means of β_1 based on 300 simulated datasets for Simulation Study 1, Scenarios 3, 4, 5 and 6 (ordered from top to bottom). Each color represents a different prior given to the columns of Φ , namely, red for ICAR, blue for PCAR and green for BYM2.

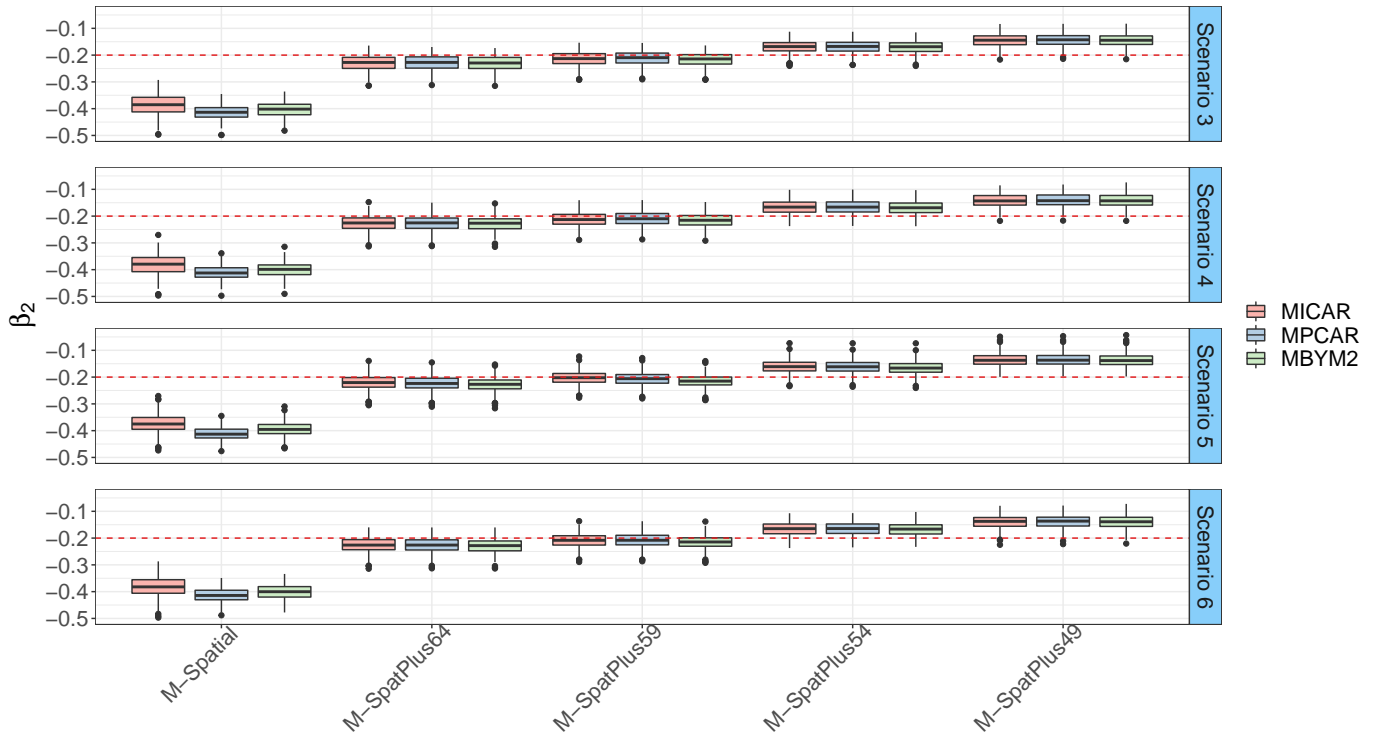


Figure A.3: Boxplots of the estimated means of β_2 based on 300 simulated datasets for Simulation Study 1, Scenarios 3, 4, 5 and 6 (ordered from top to bottom). Each color represents a different prior given to the columns of Φ , namely, red for ICAR, blue for PCAR and green for BYM2.

Table A.3: Estimated standard errors ($s.e.est$) and simulated standard errors ($s.e.sim$) for β_1 based on 300 simulated datasets for Simulation study 1 and Scenarios 1 to 6.

		ICAR		PCAR		BYM2	
	Model	$s.e.est$	$s.e.sim$	$s.e.est$	$s.e.sim$	$s.e.est$	$s.e.sim$
Scenario 1	M-Spatial	0.0674	0.0390	0.0457	0.0263	0.0534	0.0289
	M-SpatPlus64	0.0446	0.0279	0.0429	0.0272	0.0433	0.0267
	M-SpatPlus59	0.0419	0.0267	0.0407	0.0261	0.0415	0.0255
	M-SpatPlus54	0.0407	0.0264	0.0402	0.0262	0.0420	0.0259
	M-SpatPlus49	0.0399	0.0264	0.0398	0.0262	0.0419	0.0262
Scenario 2	M-Spatial	0.0733	0.0401	0.0477	0.0265	0.0579	0.0307
	M-SpatPlus64	0.0481	0.0275	0.0449	0.0270	0.0452	0.0268
	M-SpatPlus59	0.0453	0.0263	0.0431	0.0262	0.0440	0.0257
	M-SpatPlus54	0.0431	0.0251	0.0422	0.0252	0.0443	0.0251
	M-SpatPlus49	0.0419	0.0246	0.0416	0.0246	0.0442	0.0245
Scenario 3	M-Spatial	0.0684	0.0419	0.0457	0.0272	0.0552	0.0312
	M-SpatPlus64	0.0456	0.0293	0.0423	0.0287	0.0432	0.0282
	M-SpatPlus59	0.0430	0.0280	0.0406	0.0277	0.0417	0.0270
	M-SpatPlus54	0.0416	0.0278	0.0403	0.0278	0.0422	0.0277
	M-SpatPlus49	0.0407	0.0273	0.0399	0.0273	0.0421	0.0273
Scenario 4	M-Spatial	0.0734	0.0421	0.0476	0.0259	0.0583	0.0306
	M-SpatPlus64	0.0482	0.0292	0.0438	0.0284	0.0446	0.0280
	M-Spatplus59	0.0454	0.0285	0.0418	0.0281	0.0432	0.0279
	M-SpatPlus54	0.0430	0.0270	0.0407	0.0268	0.0429	0.0271
	M-SpatPlus49	0.0418	0.0260	0.0401	0.0257	0.0427	0.0261
Scenario 5	M-Spatial	0.0773	0.0346	0.0487	0.0252	0.0567	0.0270
	M-SpatPlus64	0.0489	0.0247	0.0488	0.0244	0.0463	0.0237
	M-SpatPlus59	0.0461	0.0239	0.0464	0.0237	0.0448	0.0230
	M-SpatPlus54	0.0421	0.0229	0.0423	0.0228	0.0433	0.0227
	M-SpatPlus49	0.0407	0.0237	0.0408	0.0237	0.0428	0.0237
Scenario 6	M-Spatial	0.0737	0.0375	0.0482	0.0267	0.0580	0.0287
	M-SpatPlus64	0.0476	0.0258	0.0445	0.0251	0.0453	0.0247
	M-SpatPlus59	0.0447	0.0248	0.0422	0.0245	0.0437	0.0240
	M-SpatPlus54	0.0417	0.0231	0.0401	0.0228	0.0426	0.0226
	M-SpatPlus49	0.0404	0.0236	0.0390	0.0234	0.0421	0.0234

Table A.4: Estimated standard errors ($s.e.est$) and simulated standard errors ($s.e.sim$) for β_2 based on 300 simulated datasets for Simulation study 1 and Scenarios 1 to 6.

		ICAR		PCAR		BYM2	
	Model	$s.e.est$	$s.e.sim$	$s.e.est$	$s.e.sim$	$s.e.est$	$s.e.sim$
Scenario 1	M-Spatial	0.0596	0.0357	0.0407	0.0243	0.0462	0.0262
	M-SpatPlus64	0.0429	0.0268	0.0454	0.0267	0.0438	0.0259
	M-SpatPlus59	0.0408	0.0257	0.0432	0.0256	0.0423	0.0248
	M-SpatPlus54	0.0396	0.0252	0.0421	0.0252	0.0424	0.0251
	M-SpatPlus49	0.0393	0.0242	0.0417	0.0243	0.0426	0.0242
Scenario 2	M-Spatial	0.0690	0.0382	0.0443	0.0252	0.0508	0.0273
	M-SpatPlus64	0.0465	0.0263	0.0477	0.0256	0.0459	0.0244
	M-SpatPlus59	0.0438	0.0252	0.0452	0.0245	0.0443	0.0237
	M-SpatPlus54	0.0418	0.0242	0.0439	0.0240	0.0445	0.0236
	M-SpatPlus49	0.0411	0.0239	0.0434	0.0239	0.0447	0.0237
Scenario 3	M-Spatial	0.0593	0.0385	0.0401	0.0265	0.0454	0.0284
	M-SpatPlus64	0.0424	0.0279	0.0442	0.0277	0.0435	0.0271
	M-SpatPlus59	0.0403	0.0258	0.0421	0.0256	0.0420	0.0248
	M-SpatPlus54	0.0392	0.0248	0.0417	0.0246	0.0422	0.0243
	M-SpatPlus49	0.0389	0.0243	0.0414	0.0243	0.0424	0.0242
Scenario 4	M-Spatial	0.0597	0.0391	0.0403	0.0266	0.0453	0.0286
	M-SpatPlus64	0.0426	0.0280	0.0452	0.0282	0.0440	0.0270
	M-SpatPlus59	0.0405	0.0262	0.0430	0.0261	0.0425	0.0250
	M-SpatPlus54	0.0394	0.0258	0.0423	0.0259	0.0432	0.0254
	M-SpatPlus49	0.0391	0.0247	0.0420	0.0249	0.0434	0.0246
Scenario 5	M-Spatial	0.0607	0.0354	0.0402	0.0262	0.0455	0.0287
	M-SpatPlus64	0.0454	0.0281	0.0477	0.0278	0.0440	0.0268
	M-SpatPlus59	0.0430	0.0262	0.0456	0.0260	0.0426	0.0250
	M-SpatPlus54	0.0415	0.0256	0.0443	0.0255	0.0437	0.0252
	M-SpatPlus49	0.0411	0.0248	0.0439	0.0248	0.0443	0.0247
Scenario 6	M-Spatial	0.0590	0.0383	0.0401	0.0264	0.0453	0.0285
	M-SpatPlus64	0.0428	0.0276	0.0461	0.0277	0.0437	0.0266
	M-SpatPlus59	0.0407	0.0261	0.0438	0.0263	0.0423	0.0251
	M-SpatPlus54	0.0396	0.0253	0.0432	0.0252	0.0433	0.0249
	M-SpatPlus49	0.0393	0.0250	0.0430	0.0249	0.0438	0.0249

Table A.5: Empirical 95% coverage probabilities of the true value of β_1 and β_2 based on 300 simulated datasets for Simulation study 1 and Scenarios 3, 4, 5 and 6.

		β_1			β_2		
	Model	ICAR	PCAR	BYM2	ICAR	PCAR	BYM2
Scenario 3	M-Spatial	19.3333	0.0000	6.0000	5.0000	0.0000	0.0000
	M-SpatPlus64	90.6667	87.3333	87.0000	96.0000	98.0000	97.3333
	M-SpatPlus59	94.6667	90.0000	89.3333	98.6667	99.3333	99.0000
	M-SpatPlus54	99.6667	99.6667	100.0000	96.6667	97.3333	99.0000
	M-SpatPlus49	98.3333	98.6667	99.0000	78.0000	82.3333	86.0000
Scenario 4	M-Spatial	70.6667	26.3333	56.0000	6.0000	0.0000	0.0000
	M-SpatPlus64	99.6667	98.3333	98.3333	96.6667	97.6667	97.3333
	M-SpatPlus59	99.6667	98.6667	98.3333	99.6667	99.6667	99.6667
	M-SpatPlus54	98.0000	96.6667	97.6667	94.0000	95.3333	97.6667
	M-SpatPlus49	95.3333	95.6667	97.0000	75.0000	79.6667	84.6667
Scenario 5	M-Spatial	100.0000	100.0000	100.0000	9.0000	0.0000	0.0000
	M-SpatPlus64	64.3333	72.6667	73.6667	98.0000	98.3333	97.3333
	M-SpatPlus59	61.0000	72.6667	81.6667	100.0000	100.0000	99.3333
	M-SpatPlus54	12.0000	13.6667	20.3333	94.3333	96.6667	98.0000
	M-SpatPlus49	2.0000	3.0000	6.0000	76.6667	79.6667	83.0000
Scenario 6	M-Spatial	100.0000	99.3333	100.0000	6.3333	0.0000	0.0000
	M-SpatPlus64	96.0000	95.6667	98.0000	97.6667	97.6667	98.3333
	M-SpatPlus59	96.3333	96.6667	100.0000	99.0000	100.0000	98.6667
	M-SpatPlus54	49.6667	49.3333	60.0000	94.6667	97.0000	98.0000
	M-SpatPlus49	34.0000	31.6667	42.0000	75.3333	82.3333	85.6667

Table A.6: Posterior medians and 95% credible intervals of estimated correlations between crime 1 and crime 2 based on 300 simulated datasets for Simulation study 1 and Scenarios 3, 4, 5 and 6.

	Model	ICAR		PCAR		BYM2	
		Median	95% CI	Median	95% CI	Median	95% CI
Scenario 3	M-Spatial	0.2568	-0.2346 0.6783	0.2359	-0.1913 0.6168	0.3250	-0.2218 0.7265
	M-SpatPlus64	0.3574	-0.0573 0.7085	0.2969	0.0897 0.5364	0.7132	0.4062 0.8911
	M-SpatPlus59	0.3508	-0.0646 0.7041	0.2907	0.0839 0.5267	0.7183	0.4157 0.8902
	M-SpatPlus54	0.4754	0.1048 0.7708	0.4119	0.1556 0.6710	0.8001	0.5474 0.9283
	M-SpatPlus49	0.5076	0.1522 0.7859	0.4444	0.1718 0.7044	0.8170	0.5824 0.9340
Scenario 4	M-Spatial	0.0977	-0.3660 0.5370	0.1147	-0.3026 0.5084	0.2039	-0.3156 0.6323
	M-SpatPlus64	0.1841	-0.2184 0.5602	0.1142	-0.0361 0.2907	0.5070	0.1514 0.7525
	M-SpatPlus59	0.1716	-0.2322 0.5512	0.1096	-0.0375 0.2842	0.5073	0.1549 0.7534
	M-SpatPlus54	0.3030	-0.0723 0.6349	0.2212	0.0377 0.4361	0.6889	0.3719 0.8736
	M-SpatPlus49	0.3341	-0.0300 0.6511	0.2651	0.0557 0.5018	0.7168	0.4094 0.8884
Scenario 5	M-Spatial	0.9673	0.8510 0.9956	0.9459	0.7517 0.9947	0.9169	0.6412 0.9838
	M-SpatPlus64	0.8722	0.6981 0.9579	0.8538	0.6599 0.9515	0.7170	0.3678 0.9076
	M-SpatPlus59	0.8590	0.6711 0.9531	0.8370	0.6308 0.9461	0.6915	0.3197 0.8990
	M-SpatPlus54	0.8760	0.7030 0.9608	0.8519	0.6545 0.9527	0.7632	0.4212 0.9302
	M-SpatPlus49	0.8789	0.7100 0.9622	0.8511	0.6530 0.9534	0.7805	0.4544 0.9355
Scenario 6	M-Spatial	0.5144	0.0786 0.8245	0.4409	0.0438 0.7526	0.4642	0.0033 0.7998
	M-SpatPlus64	0.4467	0.0635 0.7441	0.3093	0.0435 0.5584	0.4428	0.0502 0.7570
	M-SpatPlus59	0.4150	0.0252 0.7239	0.2605	0.0115 0.5027	0.4133	0.0361 0.7198
	M-SpatPlus54	0.5037	0.1515 0.7727	0.3616	0.0993 0.6140	0.5861	0.1926 0.8397
	M-SpatPlus49	0.5133	0.1715 0.7757	0.3696	0.1047 0.6226	0.6180	0.2255 0.8573

Table A.7: DIC and WAIC based on 300 simulated data sets for Simulation Study 1 and Scenarios 3, 4, 5 and 6.

		ICAR		PCAR		BYM2	
	Model	DIC	WAIC	DIC	WAIC	DIC	WAIC
Scenario 3	M-Spatial	953.3899	959.0199	944.7410	940.6010	940.0554	933.2278
	M-SpatPlus64	951.5502	952.1564	945.9650	940.6912	942.7260	932.5063
	M-SpatPlus59	951.5871	952.2058	945.7270	940.4662	942.6509	932.4621
	M-SpatPlus54	953.3013	951.8469	947.7106	939.4825	946.1554	935.1135
	M-SpatPlus49	954.0929	952.0263	948.5981	939.6678	947.0794	935.5887
Scenario 4	M-Spatial	956.4190	959.9196	948.3138	942.5435	943.8799	935.4106
	M-SpatPlus64	954.4169	952.4786	950.0634	943.0617	946.4975	933.8437
	M-SpatPlus59	954.4825	952.6663	949.9523	943.3573	946.3982	933.9363
	M-SpatPlus54	956.0888	951.8025	951.5685	941.7616	949.9328	936.6268
	M-SpatPlus49	956.8527	951.8008	952.1582	941.4476	950.8215	937.1556
Scenario 5	M-Spatial	920.6782	918.4245	917.5135	913.1496	914.1673	909.6811
	SpatPlus64	928.7485	920.9094	931.7151	921.7071	926.4891	913.7202
	SpatPlus59	930.9754	923.6303	933.8990	924.3162	928.5294	916.3151
	SpatPlus54	932.7776	925.6282	936.0239	927.1580	931.8094	920.4459
	SpatPlus49	934.4598	927.5054	937.6879	928.9506	933.6649	922.6290
Scenario 6	Spatial	955.1080	960.3773	946.8813	942.3910	942.3171	935.2643
	M-SpatPlus64	953.1437	952.1915	951.3409	943.9880	946.4406	934.3222
	M-SpatPlus59	953.6909	952.7222	951.3973	944.3156	946.6463	934.6044
	M-SpatPlus54	954.6095	952.1191	952.7415	943.5699	949.8364	937.4908
	M-SpatPlus49	955.5693	952.3564	953.3667	943.5717	951.0021	938.2834

Table A.8: Average value of mean absolute relative bias (MARB) and mean relative root mean prediction error (MRRMSE) of the relative risks based on 300 simulated datasets for Simulation study 1 and Scenarios 1 to 6.

	Model	ICAR		PCAR		BYM2	
		MARB	MRRMSE	MARB	MRRMSE	MARB	MRRMSE
Scenario 1	M-Spatial	0.0916	0.1550	0.0823	0.1507	0.0805	0.1480
	M-SpatPlus64	0.0865	0.1553	0.0804	0.1539	0.0754	0.1513
	M-SpatPlus59	0.0862	0.1554	0.0794	0.1535	0.0740	0.1509
	M-SpatPlus54	0.0834	0.1574	0.0766	0.1557	0.0736	0.1544
	M-SpatPlus49	0.0828	0.1585	0.0761	0.1566	0.0722	0.1554
Scenario 2	M-Spatial	0.0927	0.1717	0.0847	0.1673	0.0831	0.1640
	M-SpatPlus64	0.0895	0.1712	0.0828	0.1680	0.0783	0.1647
	M-SpatPlus59	0.0887	0.1709	0.0820	0.1674	0.0766	0.1638
	M-SpatPlus54	0.0858	0.1723	0.0793	0.1691	0.0756	0.1668
	M-SpatPlus49	0.0841	0.1726	0.0768	0.1692	0.0738	0.1671
Scenario 3	M-Spatial	0.0953	0.1621	0.0865	0.1570	0.0845	0.1539
	M-SpatPlus64	0.0890	0.1620	0.0830	0.1594	0.0783	0.1569
	M-SpatPlus59	0.0878	0.1618	0.0817	0.1588	0.0760	0.1562
	M-SpatPlus54	0.0856	0.1647	0.0788	0.1618	0.0758	0.1604
	M-SpatPlus49	0.0846	0.1658	0.0775	0.1626	0.0742	0.1614
Scenario 4	M-Spatial	0.0946	0.1665	0.0861	0.1614	0.0842	0.1583
	M-SpatPlus64	0.0883	0.1663	0.0834	0.1654	0.0782	0.1621
	M-SpatPlus59	0.0876	0.1663	0.0827	0.1649	0.0761	0.1614
	M-SpatPlus54	0.0857	0.1691	0.0800	0.1671	0.0766	0.1653
	M-SpatPlus49	0.0843	0.1701	0.0784	0.1677	0.0751	0.1660
Scenario 5	M-Spatial	0.0594	0.1356	0.0568	0.1340	0.0563	0.1311
	M-SpatPlus64	0.0622	0.1442	0.0626	0.1482	0.0591	0.1434
	M-SpatPlus59	0.0639	0.1466	0.0641	0.1505	0.0605	0.1458
	M-SpatPlus54	0.0661	0.1490	0.0680	0.1529	0.0647	0.1495
	M-SpatPlus49	0.0673	0.1507	0.0684	0.1545	0.0652	0.1513
Scenario 6	M-Spatial	0.0955	0.1648	0.0863	0.1601	0.0843	0.1570
	M-SpatPlus64	0.0883	0.1648	0.0827	0.1665	0.0783	0.1621
	M-SpatPlus59	0.0881	0.1654	0.0823	0.1666	0.0768	0.1623
	M-SpatPlus54	0.0866	0.1672	0.0805	0.1681	0.0778	0.1655
	M-SpatPlus49	0.0859	0.1684	0.0798	0.1687	0.0768	0.1664

Table A.9: Length of the 95% credible intervals of β_1 and β_2 based on 300 simulated datasets for Simulation study 1 and Scenarios 1 to 6.

	Model	β_1			β_2		
		ICAR	PCAR	BYM2	ICAR	PCAR	BYM2
Scenario 1	M-Spatial	0.2654	0.1801	0.2104	0.2347	0.1604	0.1820
	M-SpatPlus64	0.1755	0.1687	0.1703	0.1689	0.1786	0.1722
	M-SpatPlus59	0.1647	0.1600	0.1631	0.1604	0.1699	0.1663
	M-SpatPlus54	0.1601	0.1581	0.1652	0.1557	0.1655	0.1668
	M-SpatPlus49	0.1569	0.1563	0.1648	0.1545	0.1640	0.1676
Scenario 2	M-Spatial	0.2887	0.1879	0.2283	0.2719	0.1747	0.2002
	M-SpatPlus64	0.1895	0.1762	0.1778	0.1830	0.1872	0.1804
	M-SpatPlus59	0.1784	0.1693	0.1728	0.1725	0.1775	0.1742
	M-SpatPlus54	0.1696	0.1656	0.1742	0.1643	0.1724	0.1750
	M-SpatPlus49	0.1649	0.1634	0.1737	0.1618	0.1703	0.1758
Scenario 3	M-Spatial	0.2695	0.1801	0.2176	0.2338	0.1581	0.1790
	M-SpatPlus64	0.1797	0.1663	0.1696	0.1667	0.1736	0.1710
	M-SpatPlus59	0.1693	0.1595	0.1638	0.1585	0.1654	0.1651
	M-SpatPlus54	0.1636	0.1582	0.1658	0.1543	0.1636	0.1660
	M-SpatPlus49	0.1599	0.1568	0.1654	0.1531	0.1625	0.1666
Scenario 4	M-Spatial	0.2893	0.1877	0.2298	0.2353	0.1587	0.1784
	M-SpatPlus64	0.1896	0.1718	0.1755	0.1677	0.1776	0.1731
	M-SpatPlus59	0.1786	0.1643	0.1699	0.1592	0.1689	0.1670
	M-SpatPlus54	0.1692	0.1597	0.1687	0.1550	0.1662	0.1698
	M-SpatPlus49	0.1644	0.1574	0.1677	0.1539	0.1650	0.1705
Scenario 5	M-Spatial	0.3047	0.1918	0.2233	0.2391	0.1581	0.1793
	M-SpatPlus64	0.1928	0.1921	0.1822	0.1787	0.1876	0.1730
	M-SpatPlus59	0.1817	0.1826	0.1763	0.1690	0.1794	0.1674
	M-SpatPlus54	0.1659	0.1666	0.1705	0.1632	0.1741	0.1717
	M-SpatPlus49	0.1602	0.1605	0.1683	0.1615	0.1726	0.1743
Scenario 6	M-Spatial	0.2903	0.1901	0.2287	0.2326	0.1580	0.1784
	M-SpatPlus64	0.1876	0.1751	0.1784	0.1683	0.1812	0.1718
	M-SpatPlus59	0.1761	0.1661	0.1719	0.1600	0.1722	0.1661
	M-SpatPlus54	0.1641	0.1577	0.1676	0.1556	0.1699	0.1701
	M-SpatPlus49	0.1590	0.1533	0.1656	0.1547	0.1688	0.1723

Table A.10: Average value of mean absolute relative bias (MARB) and mean relative root mean prediction error (MRRMSE) of β_1 based on 300 simulated datasets for Simulation study 1 and Scenarios 1 to 6.

	Model	ICAR		PCAR		BYM2	
		MARB	MRRMSE	MARB	MRRMSE	MARB	MRRMSE
Scenario 1	M-Spatial	0.9972	1.0305	1.1079	1.1217	1.0322	1.0500
	M-SpatPlus64	0.2459	0.3084	0.2630	0.3196	0.2946	0.3444
	M-SpatPlus59	0.2121	0.2769	0.2421	0.2983	0.2878	0.3343
	M-SpatPlus54	0.1311	0.2195	0.1232	0.2137	0.1120	0.2057
	M-SpatPlus49	0.2394	0.2971	0.2322	0.2907	0.2255	0.2854
Scenario 2	M-Spatial	0.8046	0.8479	0.7463	0.7670	0.7264	0.7547
	M-SpatPlus64	0.1279	0.2237	0.1402	0.2284	0.1638	0.2426
	M-SpatPlus59	0.0988	0.2013	0.1298	0.2174	0.1652	0.2381
	M-SpatPlus54	0.1942	0.2564	0.1948	0.2574	0.1924	0.2550
	M-SpatPlus49	0.2693	0.3153	0.2603	0.3077	0.2607	0.3077
Scenario 3	M-Spatial	1.1380	1.1718	1.1130	1.1276	1.0868	1.1066
	M-SpatPlus64	0.3254	0.3795	0.3344	0.3852	0.3561	0.4027
	M-SpatPlus59	0.2765	0.3337	0.3006	0.3526	0.3303	0.3763
	M-SpatPlus54	0.0455	0.1906	0.0439	0.1903	0.0406	0.1894
	M-SpatPlus49	0.1411	0.2302	0.1355	0.2268	0.1329	0.2252
Scenario 4	M-Spatial	0.8138	0.8610	0.7360	0.7561	0.7309	0.7589
	M-SpatPlus64	0.1330	0.2357	0.1432	0.2374	0.1616	0.2469
	M-SpatPlus59	0.1021	0.2159	0.1293	0.2275	0.1602	0.2455
	M-SpatPlus54	0.1837	0.2571	0.1846	0.2568	0.1850	0.2586
	M-SpatPlus49	0.2552	0.3084	0.2492	0.3023	0.2498	0.3043
Scenario 5	M-Spatial	0.2884	0.3693	0.0656	0.1806	0.0929	0.2028
	M-SpatPlus64	0.5622	0.5858	0.5259	0.5504	0.4851	0.5103
	M-SpatPlus59	0.5462	0.5690	0.5051	0.5292	0.4310	0.4574
	M-SpatPlus54	0.7427	0.7582	0.7278	0.7435	0.7018	0.7179
	M-SpatPlus49	0.8300	0.8448	0.8237	0.8387	0.8132	0.8283
Scenario 6	M-Spatial	0.0866	0.2643	0.1404	0.2267	0.0758	0.2059
	M-SpatPlus64	0.3027	0.3480	0.2727	0.3198	0.2468	0.2968
	M-SpatPlus59	0.2811	0.3263	0.2234	0.2765	0.1785	0.2396
	M-SpatPlus54	0.5350	0.5568	0.5260	0.5476	0.5165	0.5380
	M-SpatPlus49	0.5939	0.6144	0.5837	0.6042	0.5798	0.6005

Table A.11: Average value of mean absolute relative bias (MARB) and mean relative root mean prediction error (MRRMSE) of β_2 based on 300 simulated datasets for Simulation study 1 and Scenarios 1 to 6.

	Model	ICAR		PCAR		BYM2	
		MARB	MRRMSE	MARB	MRRMSE	MARB	MRRMSE
Scenario 1	M-Spatial	0.9140	0.9312	1.0698	1.0767	0.9982	1.0067
	M-SpatPlus64	0.1292	0.1862	0.1266	0.1839	0.1411	0.1917
	M-SpatPlus59	0.0471	0.1369	0.0373	0.1331	0.0717	0.1431
	M-SpatPlus54	0.1685	0.2105	0.1725	0.2137	0.1615	0.2046
	M-SpatPlus49	0.2939	0.3178	0.2999	0.3236	0.2950	0.3189
Scenario 2	M-Spatial	0.5761	0.6070	0.7782	0.7883	0.7016	0.7147
	M-SpatPlus64	0.0597	0.1444	0.0577	0.1402	0.0392	0.1284
	M-SpatPlus59	0.1103	0.1676	0.1182	0.1703	0.0716	0.1383
	M-SpatPlus54	0.3160	0.3383	0.3153	0.3373	0.2983	0.3208
	M-SpatPlus49	0.4349	0.4510	0.4422	0.4581	0.4338	0.4497
Scenario 3	M-Spatial	0.9313	0.9511	1.0688	1.0770	1.0145	1.0244
	M-SpatPlus64	0.1494	0.2043	0.1448	0.2005	0.1544	0.2053
	M-SpatPlus59	0.0686	0.1463	0.0560	0.1397	0.0810	0.1481
	M-SpatPlus54	0.1535	0.1972	0.1566	0.1993	0.1472	0.1909
	M-SpatPlus49	0.2768	0.3023	0.2833	0.3083	0.2791	0.3041
Scenario 4	M-Spatial	0.9095	0.9303	1.0565	1.0648	1.0006	1.0107
	M-SpatPlus64	0.1360	0.1952	0.1334	0.1940	0.1433	0.1967
	M-SpatPlus59	0.0607	0.1442	0.0504	0.1401	0.0775	0.1469
	M-SpatPlus54	0.1656	0.2098	0.1681	0.2123	0.1574	0.2023
	M-SpatPlus49	0.2905	0.3157	0.2974	0.3225	0.2925	0.3174
Scenario 5	M-Spatial	0.8648	0.8827	1.0593	1.0674	0.9694	0.9799
	M-SpatPlus64	0.1029	0.1740	0.1202	0.1839	0.1410	0.1946
	M-SpatPlus59	0.0164	0.1322	0.0332	0.1343	0.0781	0.1472
	M-SpatPlus54	0.1932	0.2316	0.1908	0.2294	0.1702	0.2117
	M-SpatPlus49	0.3198	0.3430	0.3233	0.3462	0.3139	0.3374
Scenario 6	M-Spatial	0.9092	0.9292	1.0641	1.0722	1.0026	1.0126
	M-SpatPlus64	0.1265	0.1872	0.1296	0.1896	0.1427	0.1952
	M-SpatPlus59	0.0445	0.1379	0.0411	0.1380	0.0751	0.1464
	M-SpatPlus54	0.1724	0.2139	0.1750	0.2155	0.1613	0.2039
	M-SpatPlus49	0.3032	0.3279	0.3092	0.3334	0.3032	0.3278

B Supplementary material: Simulation study 2

This section includes some additional scenarios to complement the analysis of Simulation study 2. The data is generated following the generating models (13)-(14) with $\boldsymbol{\alpha} = (\alpha_1, \alpha_2)' = (0.12, 0.03)', \boldsymbol{\beta} = (\beta_1, \beta_2)' = (0.15, 0.20)'$ and \mathbf{X}_1^* is simulated such that its correlation with spatial effects of crime 1, $\boldsymbol{\theta}_1$, and spatial effects of crime 2, $\boldsymbol{\theta}_2$, is the desired one. Below we define the correlations between \mathbf{X}_1^* , $\boldsymbol{\theta}_1$ and $\boldsymbol{\theta}_2$ chosen in each scenario:

- **Scenario 3:** $\rho = 0.5$, $\text{cor}(\mathbf{X}_1^*, \boldsymbol{\theta}_1) = 0.5$ and $\text{cor}(\mathbf{X}_1^*, \boldsymbol{\theta}_2) = 0.7$ are chosen. This is similar to Scenario 1 but choosing medium correlation between the crimes.
- **Scenario 4:** $\rho = 0.3$, $\text{cor}(\mathbf{X}_1^*, \boldsymbol{\theta}_1) = 0.3$ and $\text{cor}(\mathbf{X}_1^*, \boldsymbol{\theta}_2) = 0.7$ are chosen.
- **Scenario 5:** $\rho = 0.3$, $\text{cor}(\mathbf{X}_1^*, \boldsymbol{\theta}_1) = 0.0$ and $\text{cor}(\mathbf{X}_1^*, \boldsymbol{\theta}_2) = 0.7$ are chosen.

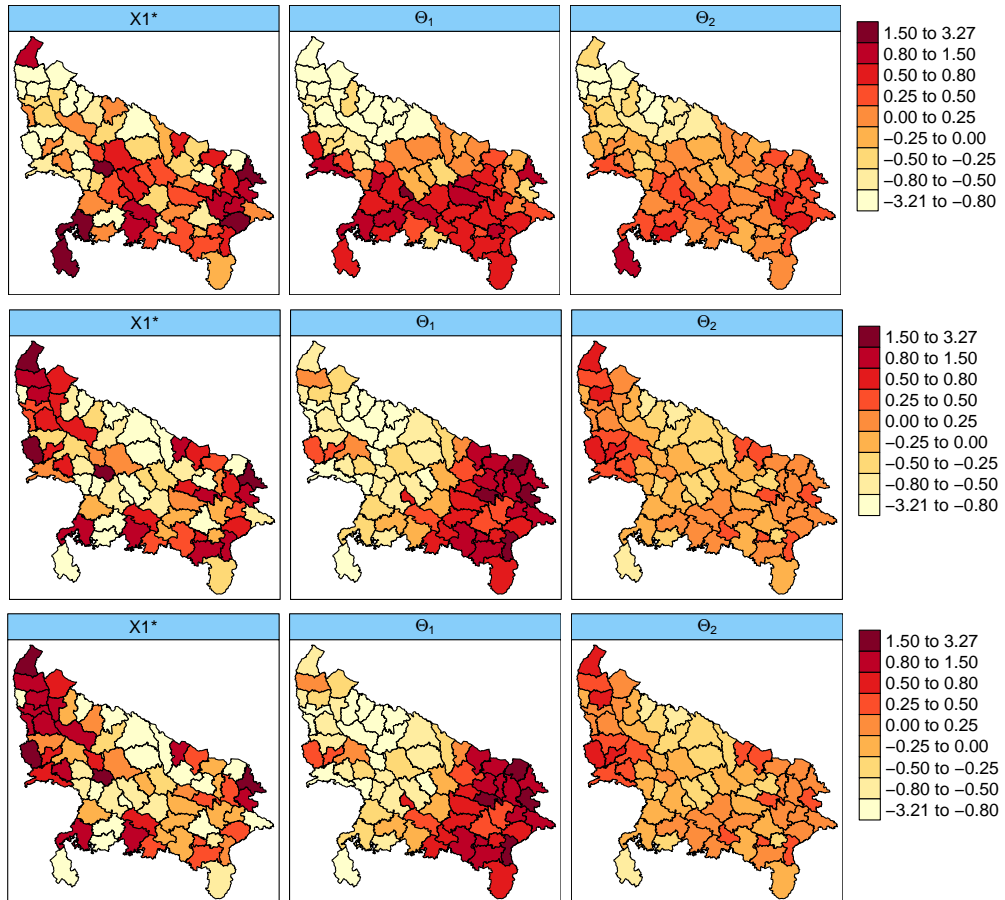


Figure B.4: From left to right, standardized simulated covariate \mathbf{X}_1^* , spatial effects $\boldsymbol{\theta}_1$ for crime 1 and spatial effects $\boldsymbol{\theta}_2$ for crime 2 in Simulation Study 2. The first row corresponds to Scenario 3, the second to Scenario 4 and the third to Scenario 5.

Table B.12: Posterior medians and 95% credible intervals of estimated correlations between crime 1 and crime 2 based on 300 simulated datasets for Simulation study 2 and Scenarios 3, 4 and 5.

	Model	ICAR			PCAR			BYM2	
		Median	95% CI	Median	95% CI	Median	95% CI	Median	95% CI
Scenario 3	M-Spatial	0.6203	0.3352	0.8260	0.6418	0.4166	0.8199	0.7990	0.5477 0.9377
	M-SpatPlus64	0.6126	0.3536	0.8014	0.6462	0.4428	0.8016	0.7140	0.4357 0.8897
	M-SpatPlus59	0.5834	0.3198	0.7797	0.6232	0.4125	0.7864	0.6801	0.3979 0.8674
	M-SpatPlus54	0.5828	0.3236	0.7758	0.6172	0.4091	0.7805	0.6834	0.3991 0.8716
	M-SpatPlus49	0.6073	0.3579	0.7920	0.6325	0.4258	0.7932	0.7046	0.4330 0.8810
	M-SpatPlus44	0.6092	0.3654	0.7900	0.6279	0.4240	0.7877	0.7168	0.4499 0.8896
	M-SpatPlus39	0.5939	0.3435	0.7810	0.6166	0.4060	0.7816	0.7076	0.4324 0.8870
Scenario 4	M-Spatial	0.4241	0.1001	0.6840	0.2636	-0.0474	0.5602	0.4675	0.1177 0.7309
	M-SpatPlus64	0.4637	0.1638	0.7025	0.3693	0.0808	0.6334	0.5192	0.2178 0.7557
	M-SpatPlus59	0.5060	0.2373	0.7170	0.4268	0.1553	0.6666	0.5622	0.2943 0.7680
	M-SpatPlus54	0.4995	0.2308	0.7115	0.4195	0.1455	0.6612	0.5566	0.2879 0.7644
	M-SpatPlus49	0.5190	0.2562	0.7248	0.4416	0.1662	0.6824	0.5738	0.3085 0.7777
	M-SpatPlus44	0.5437	0.2947	0.7387	0.4648	0.1944	0.6977	0.6016	0.3478 0.7931
	M-SpatPlus39	0.5535	0.3082	0.7448	0.4730	0.2012	0.7052	0.6144	0.3685 0.8000
Scenario 5	M-Spatial	0.5283	0.2245	0.7629	0.3750	0.0832	0.6423	0.6028	0.2939 0.8212
	M-SpatPlus64	0.4963	0.2045	0.7218	0.4127	0.1107	0.6768	0.5293	0.2380 0.7546
	M-SpatPlus59	0.5199	0.2571	0.7243	0.4543	0.1797	0.6892	0.5594	0.2950 0.7638
	M-SpatPlus54	0.5011	0.2357	0.7091	0.4350	0.1562	0.6751	0.5404	0.2738 0.7488
	M-SpatPlus49	0.5049	0.2409	0.7125	0.4391	0.1613	0.6772	0.5447	0.2798 0.7527
	M-SpatPlus44	0.5287	0.2761	0.7275	0.4650	0.1943	0.6956	0.5704	0.3157 0.7660
	M-SpatPlus39	0.5217	0.2701	0.7214	0.4528	0.1773	0.6895	0.5742	0.3167 0.7730

Table B.13: Posterior means and standard deviations of β_1 based on 300 simulated datasets for Simulation study 2 and Scenarios 3, 4 and 5.

	Model	ICAR		PCAR		BYM2		
		True value	Mean	SD	Mean	SD	Mean	SD
Scenario 3	M-Spatial	0.1500	0.2715	0.0807	0.2753	0.0813	0.2720	0.0822
	M-SpatPlus64		0.1948	0.0657	0.1921	0.0653	0.1925	0.0670
	M-SpatPlus59		0.1927	0.0626	0.1909	0.0624	0.1931	0.0641
	M-SpatPlus54		0.1758	0.0595	0.1745	0.0593	0.1764	0.0611
	M-SpatPlus49		0.1527	0.0576	0.1511	0.0575	0.1519	0.0595
	M-SpatPlus44		0.1389	0.0554	0.1379	0.0554	0.1386	0.0578
	M-SpatPlus39		0.1465	0.0538	0.1455	0.0539	0.1475	0.0563
Scenario 4	M-Spatial	0.1500	0.3082	0.0726	0.3111	0.0751	0.3149	0.0747
	M-SpatPlus64		0.2722	0.0686	0.2725	0.0709	0.2743	0.0703
	M-SpatPlus59		0.2213	0.0648	0.2193	0.0672	0.2193	0.0661
	M-SpatPlus54		0.2205	0.0632	0.2190	0.0656	0.2194	0.0646
	M-SpatPlus49		0.2018	0.0619	0.2004	0.0642	0.2005	0.0634
	M-SpatPlus44		0.1758	0.0607	0.1743	0.0630	0.1743	0.0628
	M-SpatPlus39		0.1536	0.0568	0.1527	0.0592	0.1529	0.0596
Scenario 5	M-Spatial	0.1500	0.2368	0.0776	0.2317	0.0799	0.2374	0.0792
	M-SpatPlus64		0.2096	0.0703	0.2104	0.0724	0.2111	0.0718
	M-SpatPlus59		0.1635	0.0660	0.1618	0.0682	0.1602	0.0674
	M-SpatPlus54		0.1661	0.0640	0.1648	0.0662	0.1639	0.0655
	M-SpatPlus49		0.1572	0.0624	0.1559	0.0646	0.1555	0.0641
	M-SpatPlus44		0.1312	0.0612	0.1300	0.0633	0.1288	0.0633
	M-SpatPlus39		0.1202	0.0571	0.1194	0.0593	0.1188	0.0599

Table B.14: Posterior means and standard deviations of β_2 based on 300 simulated datasets for Simulation study 2 and Scenarios 3, 4 and 5.

	Model	True value	ICAR		PCAR		BYM2	
			Mean	SD	Mean	SD	Mean	SD
Scenario 3	M-Spatial	0.2000	0.3540	0.0423	0.3788	0.0446	0.3759	0.0442
	M-SpatPlus64		0.2602	0.0381	0.2633	0.0425	0.2630	0.0412
	M-SpatPlus59		0.2402	0.0375	0.2413	0.0415	0.2401	0.0405
	M-SpatPlus54		0.2132	0.0368	0.2144	0.0407	0.2111	0.0399
	M-SpatPlus49		0.1977	0.0357	0.1998	0.0394	0.1962	0.0389
	M-SpatPlus44		0.1780	0.0359	0.1793	0.0392	0.1773	0.0397
Scenario 4	M-SpatPlus39	0.2000	0.1764	0.0350	0.1776	0.0384	0.1761	0.0389
	M-Spatial		0.3474	0.0384	0.3578	0.0398	0.3648	0.0399
	M-SpatPlus64		0.3157	0.0378	0.3177	0.0389	0.3259	0.0395
	M-SpatPlus59		0.2603	0.0391	0.2612	0.0399	0.2623	0.0409
	M-SpatPlus54		0.2479	0.0385	0.2486	0.0393	0.2491	0.0404
	M-SpatPlus49		0.2333	0.0380	0.2333	0.0387	0.2344	0.0399
Scenario 5	M-SpatPlus44	0.2000	0.2049	0.0389	0.2051	0.0395	0.2066	0.0413
	M-SpatPlus39		0.1620	0.0380	0.1623	0.0386	0.1635	0.0409
	M-Spatial		0.3707	0.0392	0.3883	0.0404	0.3899	0.0405
	M-SpatPlus64		0.3251	0.0379	0.3257	0.0388	0.3327	0.0393
	M-SpatPlus59		0.2702	0.0394	0.2704	0.0402	0.2714	0.0411
	M-SpatPlus54		0.2542	0.0387	0.2545	0.0394	0.2548	0.0404

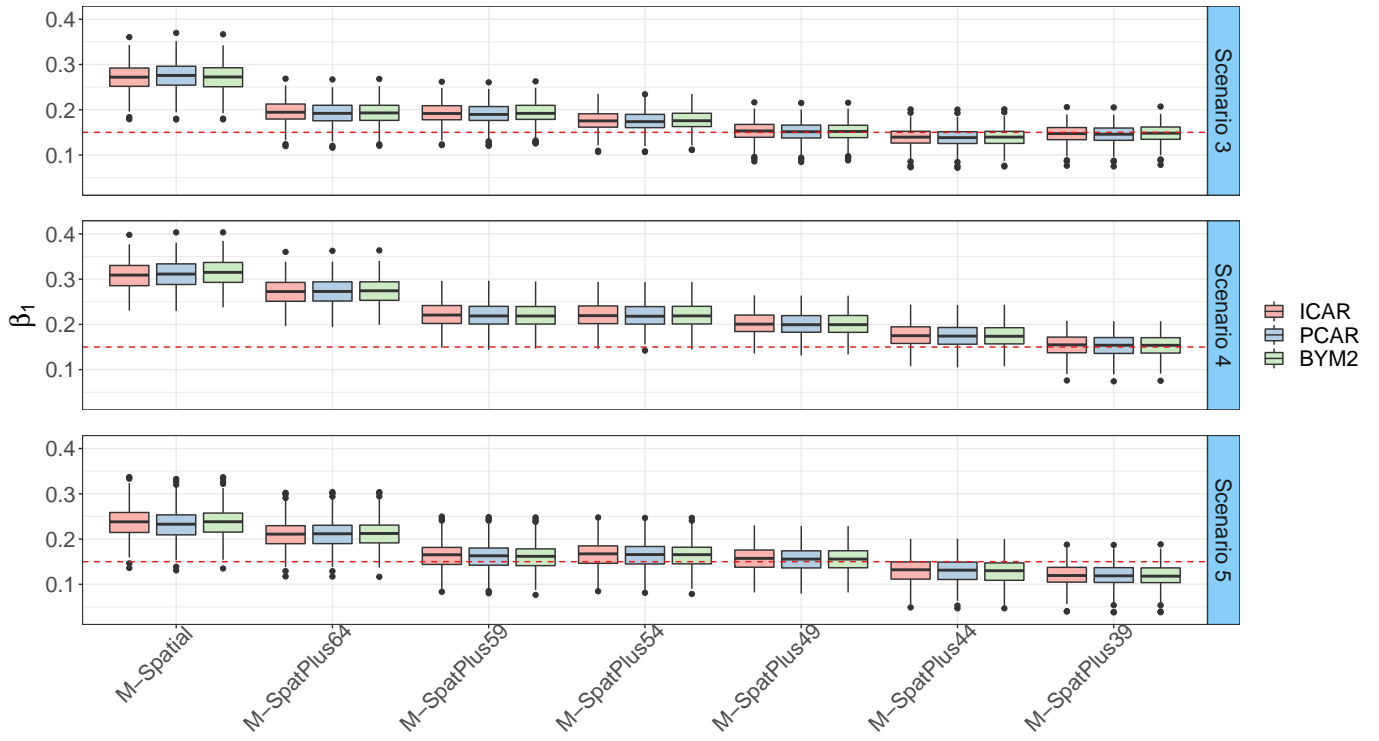


Figure B.5: Boxplots of the estimated means of β_1 based on 300 simulated datasets for Simulation Study 2, Scenarios 3, 4, 5 and 6 (ordered from top to bottom). Each color represents a different prior given to the columns of Φ , namely, red for ICAR, blue for PCAR and green for BYM2.

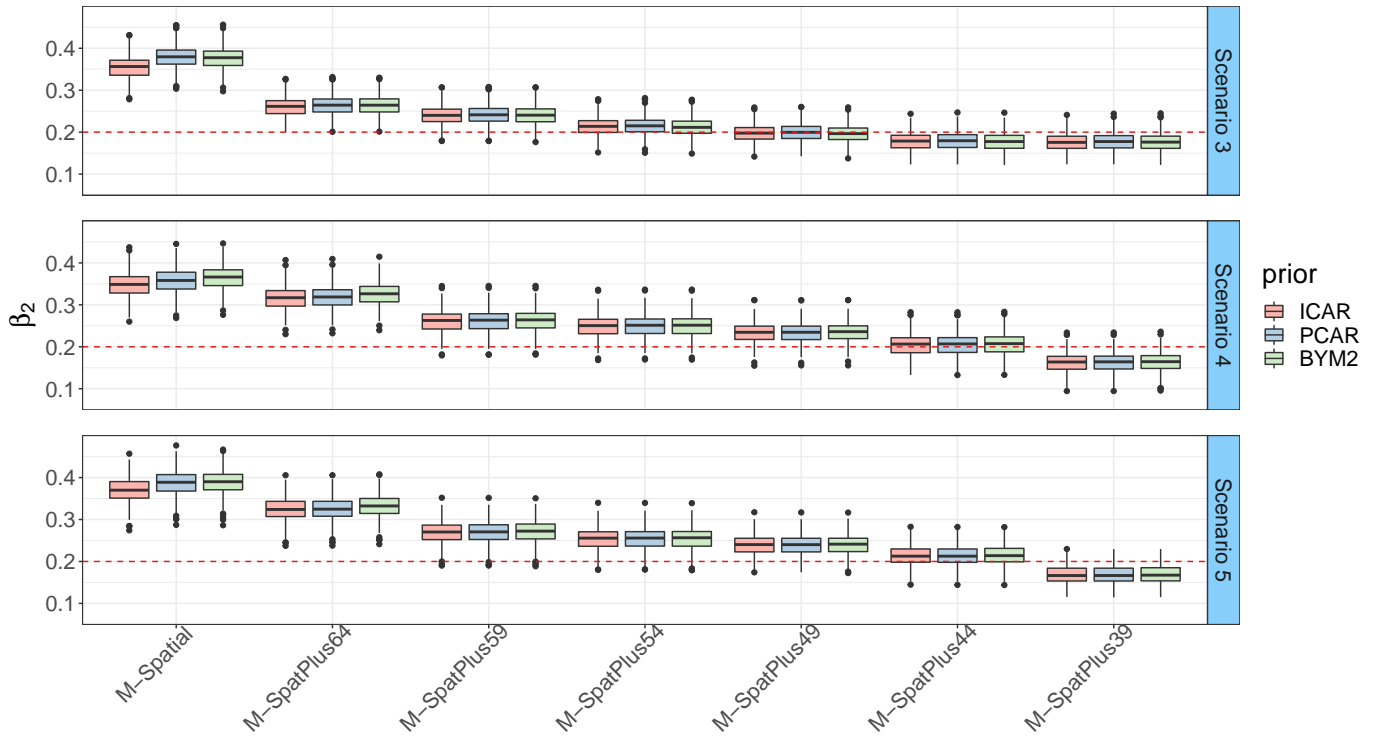


Figure B.6: Boxplots of the estimated means of β_2 based on 300 simulated datasets for Simulation Study 2, Scenarios 3, 4, 5 and 6 (ordered from top to bottom). Each color represents a different prior given to the columns of Φ , namely, red for ICAR, blue for PCAR and green for BYM2.

Table B.15: Estimated standard errors ($s.e.est$) and simulated standard errors ($s.e.sim$) for β_1 based on 300 simulated datasets for Simulation study 2 and Scenarios 1 to 5.

		ICAR		PCAR		BYM2	
	Model	$s.e.est$	$s.e.sim$	$s.e.est$	$s.e.sim$	$s.e.est$	$s.e.sim$
Scenario 1	M-Spatial	0.0815	0.0338	0.0519	0.0290	0.0846	0.0338
	M-SpatPlus64	0.0612	0.0254	0.0404	0.0214	0.0630	0.0253
	M-SpatPlus59	0.0585	0.0249	0.0393	0.0206	0.0605	0.0250
	M-SpatPlus54	0.0580	0.0242	0.0390	0.0199	0.0599	0.0242
	M-SpatPlus49	0.0563	0.0225	0.0378	0.0191	0.0584	0.0225
	M-SpatPlus44	0.0547	0.0228	0.0555	0.0228	0.0574	0.0230
Scenario 2	M-SpatPlus39	0.0517	0.0204	0.0526	0.0204	0.0549	0.0205
	M-Spatial	0.0685	0.0295	0.0712	0.0299	0.0708	0.0291
	M-SpatPlus64	0.0656	0.0283	0.0681	0.0286	0.0675	0.0280
	M-SpatPlus59	0.0640	0.0275	0.0665	0.0278	0.0656	0.0272
	M-SpatPlus54	0.0625	0.0268	0.0650	0.0271	0.0642	0.0265
	M-SpatPlus49	0.0612	0.0252	0.0636	0.0255	0.0631	0.0249
Scenario 3	M-SpatPlus44	0.0599	0.0266	0.0624	0.0268	0.0624	0.0267
	M-SpatPlus39	0.0568	0.0239	0.0593	0.0241	0.0599	0.0239
	M-Spatial	0.0807	0.0301	0.0813	0.0307	0.0822	0.0302
	M-SpatPlus64	0.0657	0.0246	0.0653	0.0245	0.0670	0.0245
	M-SpatPlus59	0.0626	0.0235	0.0624	0.0234	0.0641	0.0234
	M-SpatPlus54	0.0595	0.0222	0.0593	0.0221	0.0611	0.0221
Scenario 4	M-SpatPlus49	0.0576	0.0211	0.0575	0.0211	0.0595	0.0209
	M-SpatPlus44	0.0554	0.0208	0.0554	0.0208	0.0578	0.0207
	M-SpatPlus39	0.0538	0.0203	0.0539	0.0203	0.0563	0.0203
	M-Spatial	0.0726	0.0316	0.0751	0.0318	0.0747	0.0310
	M-SpatPlus64	0.0686	0.0300	0.0709	0.0302	0.0703	0.0296
	M-SpatPlus59	0.0648	0.0277	0.0672	0.0280	0.0661	0.0275
Scenario 5	M-SpatPlus54	0.0632	0.0269	0.0656	0.0273	0.0646	0.0268
	M-SpatPlus49	0.0619	0.0256	0.0642	0.0259	0.0634	0.0255
	M-SpatPlus44	0.0607	0.0265	0.0630	0.0268	0.0628	0.0266
	M-SpatPlus39	0.0568	0.0235	0.0592	0.0238	0.0596	0.0235
	M-Spatial	0.0776	0.0342	0.0799	0.0344	0.0792	0.0334
	M-SpatPlus64	0.0703	0.0312	0.0724	0.0315	0.0718	0.0307
	M-SpatPlus59	0.0660	0.0294	0.0682	0.0296	0.0674	0.0292
	M-SpatPlus54	0.0640	0.0285	0.0662	0.0287	0.0655	0.0283
	M-SpatPlus49	0.0624	0.0268	0.0646	0.0271	0.0641	0.0266
	M-SpatPlus44	0.0612	0.0279	0.0633	0.0281	0.0633	0.0280
	M-SpatPlus39	0.0571	0.0259	0.0593	0.0262	0.0599	0.0260

Table B.16: Estimated standard errors ($s.e._{est}$) and simulated standard errors ($s.e._{sim}$) for β_2 based on 300 simulated datasets for Simulation study 2 and Scenarios 1 to 5.

		ICAR		PCAR		BYM2	
	Model	$s.e._{est}$	$s.e._{sim}$	$s.e._{est}$	$s.e._{sim}$	$s.e._{est}$	$s.e._{sim}$
Scenario 1	M-Spatial	0.0476	0.0272	0.0519	0.0290	0.0501	0.0275
	M-SpatPlus64	0.0380	0.0210	0.0404	0.0214	0.0398	0.0211
	M-SpatPlus59	0.0370	0.0203	0.0393	0.0206	0.0388	0.0203
	M-SpatPlus54	0.0367	0.0196	0.0390	0.0199	0.0385	0.0197
	M-SpatPlus49	0.0355	0.0189	0.0378	0.0191	0.0374	0.0189
	M-SpatPlus44	0.0353	0.0199	0.0375	0.0201	0.0375	0.0201
Scenario 2	M-Spatial	0.0381	0.0285	0.0393	0.0286	0.0399	0.0279
	M-SpatPlus64	0.0371	0.0276	0.0382	0.0278	0.0392	0.0274
	M-SpatPlus59	0.0380	0.0272	0.0389	0.0273	0.0401	0.0270
	M-SpatPlus54	0.0374	0.0265	0.0383	0.0266	0.0395	0.0263
	M-SpatPlus49	0.0368	0.0258	0.0376	0.0258	0.0389	0.0256
	M-SpatPlus44	0.0378	0.0261	0.0384	0.0261	0.0404	0.0261
Scenario 3	M-Spatial	0.0423	0.0284	0.0446	0.0281	0.0442	0.0276
	M-SpatPlus64	0.0381	0.0242	0.0425	0.0250	0.0412	0.0244
	M-SpatPlus59	0.0375	0.0235	0.0415	0.0241	0.0405	0.0237
	M-SpatPlus54	0.0368	0.0222	0.0407	0.0228	0.0399	0.0224
	M-SpatPlus49	0.0357	0.0210	0.0394	0.0216	0.0389	0.0212
	M-SpatPlus44	0.0359	0.0220	0.0392	0.0223	0.0397	0.0224
Scenario 4	M-Spatial	0.0423	0.0284	0.0446	0.0281	0.0442	0.0276
	M-SpatPlus64	0.0381	0.0242	0.0425	0.0250	0.0412	0.0244
	M-SpatPlus59	0.0375	0.0235	0.0415	0.0241	0.0405	0.0237
	M-SpatPlus54	0.0368	0.0222	0.0407	0.0228	0.0399	0.0224
	M-SpatPlus49	0.0357	0.0210	0.0394	0.0216	0.0389	0.0212
	M-SpatPlus44	0.0359	0.0220	0.0392	0.0223	0.0397	0.0224
Scenario 5	M-Spatial	0.0423	0.0284	0.0446	0.0281	0.0442	0.0276
	M-SpatPlus64	0.0381	0.0242	0.0425	0.0250	0.0412	0.0244
	M-SpatPlus59	0.0375	0.0235	0.0415	0.0241	0.0405	0.0237
	M-SpatPlus54	0.0368	0.0222	0.0407	0.0228	0.0399	0.0224
	M-SpatPlus49	0.0357	0.0210	0.0394	0.0216	0.0389	0.0212
	M-SpatPlus44	0.0359	0.0220	0.0392	0.0223	0.0397	0.0224

Table B.17: Empirical 95% coverage probabilities of the true value of β_1 and β_2 based on 300 simulated datasets for Simulation study 2 and Scenarios 3, 4 and 5.

		β_1			β_2		
		ICAR	PCAR	BYM2	ICAR	PCAR	BYM2
Scenario 3	M-Spatial	88.3333	85.3333	89.3333	1.3333	0.0000	0.0000
	M-SpatPlus64	100.0000	100.0000	100.0000	73.6667	80.6667	78.0000
	M-SpatPlus59	100.0000	100.0000	100.0000	92.6667	95.6667	95.6667
	M-SpatPlus54	100.0000	100.0000	100.0000	99.0000	99.6667	99.6667
	M-SpatPlus49	100.0000	100.0000	100.0000	100.0000	100.0000	100.0000
	M-SpatPlus44	100.0000	100.0000	100.0000	98.6667	99.6667	99.6667
Scenario 4	M-SpatPlus39	100.0000	100.0000	100.0000	98.0000	99.3333	99.0000
	M-Spatial	31.6667	35.0000	28.3333	0.6667	0.6667	0.3333
	M-SpatPlus64	64.3333	68.3333	66.0000	8.0000	8.0000	4.0000
	M-SpatPlus59	98.0000	99.0000	99.0000	70.3333	72.0000	71.0000
	M-SpatPlus54	97.6667	99.0000	98.0000	88.3333	89.0000	90.6667
	M-SpatPlus49	100.0000	100.0000	100.0000	94.6667	94.6667	95.6667
Scenario 5	M-SpatPlus44	100.0000	100.0000	100.0000	99.3333	99.3333	99.3333
	M-SpatPlus39	100.0000	100.0000	100.0000	92.6667	94.0000	95.3333
	M-Spatial	96.6667	98.6667	96.6667	0.3333	0.0000	0.0000
	M-SpatPlus64	99.3333	99.3333	99.3333	2.3333	2.6667	2.0000
	M-SpatPlus59	100.0000	100.0000	100.0000	59.0000	61.0000	62.6667
	M-SpatPlus54	100.0000	100.0000	100.0000	82.0000	83.6667	85.6667
Scenario 6	M-SpatPlus49	100.0000	100.0000	100.0000	93.3333	94.0000	94.6667
	M-Spatplus44	100.0000	100.0000	100.0000	99.3333	99.3333	99.3333
	M-SpatPlus39	100.0000	100.0000	100.0000	96.6667	97.3333	98.3333

Table B.18: DIC and WAIC based on 300 simulated data sets for Simulation Study 2 and Scenarios 3, 4 and 5.

		ICAR		PCAR		BYM2	
	Model	DIC	WAIC	DIC	WAIC	DIC	WAIC
Scenario 3	M-Spatial	967.9454	954.5795	967.5495	952.1199	967.9909	951.7634
	M-SpatPlus64	969.1749	951.7115	970.9422	951.6440	970.9431	950.8905
	M-SpatPlus59	970.2056	951.4510	972.0560	951.7777	972.2680	951.2902
	M-SpatPlus54	972.2309	953.1453	973.6655	952.8703	974.4395	953.3604
	M-SpatPlus49	973.2094	954.5434	974.3598	953.7926	975.3738	954.5668
	M-SpatPlus44	974.3461	955.1660	975.2471	954.0045	976.5248	955.1149
Scenario 4	M-SpatPlus39	974.7621	955.7078	975.6728	954.5366	976.9174	955.6734
	M-Spatial	966.8835	950.9785	967.8758	948.4934	967.5878	947.7641
	M-SpatPlus64	967.1693	949.2779	968.0115	946.6388	968.0098	946.4287
	M-SpatPlus59	969.9224	948.3949	970.8501	946.1590	971.2409	947.0300
	M-SpatPlus54	970.9355	949.3026	971.8493	947.1336	972.3405	948.2459
	M-SpatPlus49	972.1451	950.7576	973.0600	948.5624	973.5596	949.7205
Scenario 5	M-SpatPlus44	974.2859	952.6960	975.0717	950.2682	975.6985	951.5074
	M-SpatPlus39	978.3585	957.7842	979.0163	955.1304	979.6206	956.2045
	M-Spatial	965.3720	950.3049	966.0718	947.7260	965.6266	946.7197
	M-SpatPlus64	965.5671	947.2383	966.5097	945.1004	966.4342	944.4985
	M-SpatPlus59	968.6013	946.5191	969.6242	944.7155	969.9139	945.2128
	M-SpatPlus54	969.9959	947.6624	971.0162	945.9452	971.4843	946.7808
	M-SpatPlus49	971.3763	949.1848	972.3350	947.4099	972.8820	948.4109
	M-SpatPlus44	973.5362	951.3029	974.4013	949.3644	975.0159	950.4543
	M-SpatPlus39	978.1803	956.8477	978.9062	954.5679	979.5386	955.6113

Table B.19: Average value of mean absolute relative bias (MARB) and mean relative root mean prediction error (MRRMSE) of the relative risks based on 300 simulated datasets for Simulation study 2 and Scenarios 1 to 5.

	Model	ICAR		PCAR		BYM2	
		MARB	MRRMSE	MARB	MRRMSE	MARB	MRRMSE
Scenario 1	M-Spatial	0.0675	0.1550	0.0649	0.1567	0.0639	0.1557
	M-SpatPlus64	0.0652	0.1567	0.0632	0.1585	0.0626	0.1579
	M-SpatPlus59	0.0660	0.1579	0.0643	0.1597	0.0642	0.1592
	M-SpatPlus54	0.0657	0.1583	0.0638	0.1601	0.0639	0.1598
	M-SpatPlus49	0.0694	0.1608	0.0671	0.1623	0.0676	0.1622
	M-SpatPlus44	0.0695	0.1612	0.0671	0.1626	0.0677	0.1626
	M-SpatPlus39	0.0737	0.1655	0.0705	0.1666	0.0715	0.1669
Scenario 2	M-Spatial	0.0634	0.1580	0.0597	0.1597	0.0602	0.1594
	M-SpatPlus64	0.0623	0.1585	0.0584	0.1601	0.0589	0.1598
	M-SpatPlus59	0.0608	0.1606	0.0571	0.1621	0.0583	0.1621
	M-SpatPlus54	0.0616	0.1615	0.0580	0.1630	0.0593	0.1630
	M-SpatPlus49	0.0622	0.1632	0.0593	0.1646	0.0601	0.1647
	M-SpatPlus44	0.0616	0.1649	0.0588	0.1663	0.0595	0.1664
	M-SpatPlus39	0.0685	0.1705	0.0651	0.1718	0.0657	0.1718
Scenario 3	M-Spatial	0.0668	0.1545	0.0647	0.1555	0.0650	0.1555
	M-SpatPlus64	0.0625	0.1571	0.0614	0.1598	0.0608	0.1592
	M-SpatPlus59	0.0618	0.1584	0.0617	0.1612	0.0609	0.1608
	M-SpatPlus54	0.0633	0.1612	0.0624	0.1634	0.0627	0.1637
	M-SpatPlus49	0.0669	0.1641	0.0650	0.1657	0.0659	0.1665
	M-SpatPlus44	0.0652	0.1648	0.0637	0.1663	0.0644	0.1673
	M-SpatPlus39	0.0674	0.1661	0.0654	0.1674	0.0665	0.1684
Scenario 4	M-Spatial	0.0621	0.1540	0.0588	0.1557	0.0596	0.1554
	M-SpatPlus64	0.0600	0.1552	0.0564	0.1569	0.0572	0.1566
	M-SpatPlus59	0.0586	0.1596	0.0550	0.1612	0.0569	0.1612
	M-SpatPlus54	0.0595	0.1608	0.0559	0.1623	0.0578	0.1625
	M-SpatPlus49	0.0608	0.1627	0.0578	0.1642	0.0594	0.1643
	M-SpatPlus44	0.0602	0.1643	0.0570	0.1657	0.0584	0.1659
	M-SpatPlus39	0.0691	0.1706	0.0654	0.1718	0.0665	0.1719
Scenario 5	M-Spatial	0.0594	0.1511	0.0571	0.1528	0.0574	0.1524
	M-SpatPlus64	0.0559	0.1527	0.0534	0.1545	0.0536	0.1543
	M-SpatPlus59	0.0547	0.1573	0.0519	0.1589	0.0532	0.1590
	M-SpatPlus54	0.0559	0.1590	0.0533	0.1606	0.0548	0.1608
	M-SpatPlus49	0.0575	0.1606	0.0550	0.1622	0.0565	0.1625
	M-SpatPlus44	0.0564	0.1625	0.0539	0.1640	0.0554	0.1643
	M-SpatPlus39	0.0642	0.1688	0.0611	0.1701	0.0624	0.1703

Table B.20: Length of the 95% credible intervals of β_1 and β_2 based on 300 simulated datasets for Simulation study 2 and Scenarios 1 to 5.

	Model	β_1			β_2		
		ICAR	PCAR	BYM2	ICAR	PCAR	BYM2
Scenario 1	M-Spatial	0.3208	0.3293	0.3328	0.1871	0.2039	0.1972
	M-SpatPlus64	0.2407	0.2435	0.2478	0.1495	0.1587	0.1565
	M-SpatPlus59	0.2304	0.2331	0.2382	0.1455	0.1546	0.1527
	M-SpatPlus54	0.2280	0.2309	0.2358	0.1443	0.1534	0.1516
	M-SpatPlus49	0.2215	0.2245	0.2298	0.1395	0.1485	0.1469
	M-SpatPlus44	0.2154	0.2184	0.2259	0.1389	0.1474	0.1476
Scenario 2	M-SpatPlus39	0.2036	0.2067	0.2161	0.1341	0.1429	0.1442
	M-Spatial	0.2694	0.2800	0.2785	0.1499	0.1543	0.1569
	M-SpatPlus64	0.2579	0.2678	0.2655	0.1460	0.1502	0.1542
	M-SpatPlus59	0.2515	0.2615	0.2582	0.1495	0.1530	0.1575
	M-SpatPlus54	0.2457	0.2555	0.2524	0.1472	0.1505	0.1552
	M-SpatPlus49	0.2408	0.2503	0.2481	0.1448	0.1478	0.1531
Scenario 3	M-SpatPlus44	0.2355	0.2453	0.2455	0.1485	0.1509	0.1588
	M-SpatPlus39	0.2232	0.2331	0.2358	0.1467	0.1488	0.1588
	M-Spatial	0.3175	0.3197	0.3234	0.1664	0.1753	0.1736
	M-SpatPlus64	0.2584	0.2567	0.2635	0.1499	0.1671	0.1619
	M-SpatPlus59	0.2464	0.2452	0.2522	0.1474	0.1632	0.1591
	M-SpatPlus54	0.2341	0.2330	0.2404	0.1445	0.1598	0.1570
Scenario 4	M-SpatPlus49	0.2266	0.2261	0.2340	0.1402	0.1547	0.1531
	M-SpatPlus44	0.2179	0.2178	0.2274	0.1410	0.1540	0.1560
	M-SpatPlus39	0.2118	0.2118	0.2215	0.1377	0.1509	0.1532
	M-Spatial	0.2855	0.2953	0.2940	0.1509	0.1566	0.1570
	M-SpatPlus64	0.2699	0.2788	0.2764	0.1486	0.1530	0.1554
	M-SpatPlus59	0.2547	0.2641	0.2601	0.1535	0.1568	0.1608
Scenario 5	M-SpatPlus54	0.2486	0.2579	0.2541	0.1514	0.1546	0.1589
	M-SpatPlus49	0.2434	0.2525	0.2494	0.1492	0.1522	0.1570
	M-SpatPlus44	0.2385	0.2477	0.2471	0.1529	0.1554	0.1625
	M-SpatPlus39	0.2234	0.2327	0.2346	0.1494	0.1517	0.1610
	M-Spatial	0.3051	0.3141	0.3113	0.1540	0.1585	0.1592
	M-SpatPlus64	0.2764	0.2849	0.2825	0.1488	0.1526	0.1544
	M-SpatPlus59	0.2595	0.2683	0.2650	0.1548	0.1579	0.1614
	M-SpatPlus54	0.2515	0.2602	0.2576	0.1520	0.1550	0.1589
	M-SpatPlus49	0.2456	0.2539	0.2521	0.1501	0.1531	0.1572
	M-SpatPlus44	0.2405	0.2489	0.2490	0.1534	0.1560	0.1621
	M-SpatPlus39	0.2246	0.2332	0.2356	0.1507	0.1534	0.1618

Table B.21: Average value of mean absolute relative bias (MARB) and mean relative root mean prediction error (MRRMSE) of β_1 based on 300 simulated datasets for Simulation study 2 and Scenarios 1 to 5.

		ICAR		PCAR		BYM2	
	Model	MARB	MRRMSE	MARB	MRRMSE	MARB	MRRMSE
Scenario 1	M-Spatial	0.8006	0.8317	0.8439	0.8738	0.8399	0.8696
	M-SpatPlus64	0.2523	0.3038	0.2473	0.2997	0.2635	0.3130
	M-SpatPlus59	0.2762	0.3223	0.2766	0.3227	0.3076	0.3500
	M-SpatPlus54	0.1391	0.2129	0.1365	0.2114	0.1541	0.2233
	M-SpatPlus49	0.0534	0.1595	0.0527	0.1594	0.0663	0.1642
	M-SpatPlus44	0.0632	0.1645	0.0618	0.1642	0.0499	0.1611
Scenario 2	M-SpatPlus39	0.1601	0.2101	0.1598	0.2100	0.1407	0.1961
	M-Spatial	0.7923	0.8164	0.8174	0.8414	0.8222	0.8448
	M-SpatPlus64	0.6038	0.6326	0.5998	0.6295	0.6044	0.6326
	M-SpatPlus59	0.4398	0.4764	0.4267	0.4652	0.4265	0.4635
	M-SpatPlus54	0.4486	0.4828	0.4380	0.4738	0.4424	0.4765
	M-SpatPlus49	0.3310	0.3712	0.3216	0.3637	0.3233	0.3635
Scenario 3	M-SpatPlus44	0.1332	0.2217	0.1235	0.2174	0.1222	0.2156
	M-SpatPlus39	0.0304	0.1623	0.0368	0.1651	0.0395	0.1639
	M-Spatial	0.8103	0.8347	0.8355	0.8602	0.8133	0.8378
	M-SpatPlus64	0.2987	0.3408	0.2809	0.3250	0.2833	0.3270
	M-SpatPlus59	0.2849	0.3251	0.2730	0.3144	0.2871	0.3267
	M-SpatPlus54	0.1723	0.2271	0.1634	0.2199	0.1762	0.2295
Scenario 4	M-SpatPlus49	0.0178	0.1415	0.0074	0.1406	0.0129	0.1400
	M-SpatPlus44	0.0739	0.1570	0.0810	0.1604	0.0761	0.1578
	M-SpatPlus39	0.0235	0.1376	0.0299	0.1387	0.0164	0.1360
	M-Spatial	1.0548	1.0756	1.0739	1.0947	1.0995	1.1188
	M-SpatPlus64	0.8148	0.8390	0.8169	0.8414	0.8285	0.8518
	M-SpatPlus59	0.4753	0.5099	0.4623	0.4986	0.4622	0.4973
Scenario 5	M-SpatPlus54	0.4700	0.5032	0.4598	0.4944	0.4627	0.4960
	M-SpatPlus49	0.3457	0.3855	0.3359	0.3778	0.3368	0.3774
	M-SpatPlus44	0.1719	0.2464	0.1623	0.2411	0.1619	0.2401
	M-SpatPlus39	0.0240	0.1585	0.0178	0.1596	0.0193	0.1579
	M-Spatial	0.5787	0.6219	0.5447	0.5910	0.5826	0.6238
	M-SpatPlus64	0.3976	0.4488	0.4029	0.4542	0.4070	0.4557
Scenario 5	M-SpatPlus59	0.0902	0.2156	0.0787	0.2125	0.0678	0.2060
	M-SpatPlus54	0.1071	0.2178	0.0984	0.2151	0.0926	0.2102
	M-SpatPlus49	0.0482	0.1852	0.0392	0.1846	0.0369	0.1814
	M-SpatPlus44	0.1255	0.2244	0.1332	0.2299	0.1413	0.2339
	M-SpatPlus39	0.1989	0.2636	0.2041	0.2685	0.2077	0.2704

Table B.22: Average value of mean absolute relative bias (MARB) and mean relative root mean prediction error (MRRMSE) of β_2 based on 300 simulated datasets for Simulation study 2 and Scenarios 1 to 5.

		ICAR		PCAR		BYM2	
	Model	MARB	MRRMSE	MARB	MRRMSE	MARB	MRRMSE
Scenario 1	M-Spatial	0.5088	0.5267	0.6421	0.6583	0.5893	0.6051
	M-SpatPlus64	0.0274	0.1087	0.0255	0.1098	0.0345	0.1109
	M-SpatPlus59	0.0309	0.1061	0.0327	0.1081	0.0263	0.1050
	M-SpatPlus54	0.0854	0.1301	0.0856	0.1314	0.0850	0.1300
	M-SpatPlus49	0.1297	0.1604	0.1303	0.1616	0.1277	0.1587
	M-SpatPlus44	0.1976	0.2213	0.2003	0.2241	0.1936	0.2181
Scenario 2	M-SpatPlus39	0.3479	0.3599	0.3492	0.3614	0.3440	0.3564
	M-Spatial	0.4378	0.4603	0.4570	0.4789	0.4984	0.5175
	M-SpatPlus64	0.3371	0.3643	0.3471	0.3738	0.3855	0.4091
	M-SpatPlus59	0.1968	0.2392	0.2017	0.2436	0.2116	0.2509
	M-SpatPlus54	0.1568	0.2053	0.1616	0.2092	0.1683	0.2134
	M-SpatPlus49	0.0945	0.1599	0.0949	0.1601	0.1065	0.1666
Scenario 3	M-SpatPlus44	0.0619	0.1445	0.0601	0.1436	0.0474	0.1391
	M-SpatPlus39	0.2732	0.3009	0.2709	0.2988	0.2641	0.2931
	M-Spatial	0.7698	0.7827	0.8939	0.9049	0.8795	0.8902
	M-SpatPlus64	0.3011	0.3245	0.3167	0.3406	0.3150	0.3377
	M-SpatPlus59	0.2010	0.2327	0.2063	0.2390	0.2004	0.2329
	M-SpatPlus54	0.0659	0.1289	0.0721	0.1349	0.0556	0.1250
Scenario 4	M-SpatPlus49	0.0115	0.1057	0.0009	0.1080	0.0188	0.1079
	M-SpatPlus44	0.1098	0.1553	0.1034	0.1522	0.1133	0.1592
	M-SpatPlus39	0.1181	0.1606	0.1122	0.1574	0.1193	0.1630
	M-Spatial	0.7372	0.7513	0.7891	0.8029	0.8242	0.8360
	M-SpatPlus64	0.5784	0.5950	0.5887	0.6051	0.6296	0.6442
	M-SpatPlus59	0.3016	0.3298	0.3060	0.3340	0.3115	0.3385
Scenario 5	M-SpatPlus54	0.2395	0.2732	0.2430	0.2763	0.2454	0.2779
	M-SpatPlus49	0.1667	0.2094	0.1664	0.2093	0.1722	0.2133
	M-SpatPlus44	0.0244	0.1333	0.0257	0.1335	0.0329	0.1348
	M-SpatPlus39	0.1900	0.2256	0.1884	0.2242	0.1827	0.2198
	M-Spatial	0.8536	0.8657	0.9415	0.9531	0.9496	0.9602
	M-SpatPlus64	0.6253	0.6399	0.6285	0.6431	0.6637	0.6774
	M-SpatPlus59	0.3510	0.3747	0.3518	0.3756	0.3568	0.3804
	M-SpatPlus54	0.2712	0.2992	0.2725	0.3005	0.2739	0.3019
	M-SpatPlus49	0.1982	0.2316	0.1973	0.2309	0.2004	0.2336
	M-SpatPlus44	0.0699	0.1394	0.0696	0.1393	0.0749	0.1426
	M-SpatPlus39	0.1601	0.1950	0.1600	0.1949	0.1555	0.1917